Properties of cryogenic and low temperature composite materials – A review

Zsombor Sápi[a], Richard Butler[a*]

[a] Materials and Structures Research Centre, Department of Mechanical Engineering, University of Bath, Claverton Down, Bath, BA2 7AY, United Kingdom

Abstract

This paper reviews the literature published since 1994 related to the behaviour of composite materials at low and cryogenic temperatures. The material properties addressed are: tensile, compressive and shear strength, elastic modulus and stress-strain behaviour; mechanical and thermal fatigue response; fracture toughness; impact resistance; thermal expansion and thermal conductivity; tribology and wear; permeability. The underlying physical principles responsible for the behaviour at cold temperatures are also discussed. Finally, the challenges related to cryogenic experimental testing are introduced.

Keywords

Microcracking; Carbon fibre; Cold temperature; Space applications; Liquid nitrogen (LN2)

[*] Corresponding author. E-mail address: R.Butler@bath.ac.uk

Contents

Nomenclature

AF	Aramid fibre
BMI	Bismaleimide
CF	Carbon fibre
CFRP	Carbon fibre reinforced polymer
COPV	Composite overwrapped pressure vessel
CT	Cryogenic temperature
CTE	Coefficient of thermal expansion
DCPD	Dicyclopentadiene
E	Elastic modulus
E_B	Absorbed energy
E_F	Flexural modulus
E_1	Longitudinal elastic modulus
E_{1C}	Longitudinal elastic modulus in compression
E_{1T}	Longitudinal elastic modulus in tension
E_2	Transverse elastic modulus
E_{2C}	Transverse elastic modulus in compression
E_{2T}	Transverse elastic modulus in tension

E_{3T}	Out-of-plane elastic modulus in tension
G_C	Critical strain energy release rate
GF	Glass fibre
GFRP	Glass fibre reinforced polymer
G_n	Strain energy release rate, $n = I, II, III$ referring to mode I, II and III
G_{nC}	Critical strain energy release rate, $n = I, II, III$ referring to mode I, II and III
G_{TC}	Total critical strain energy release rate
G_{12}	Shear modulus in plane 12
HT	High temperature
I	Impact strength
ILSS	Interlaminar shear strength
IPSS	In-plane shear strength
K_{IC}	Mode I fracture toughness
LCH_4	Liquid methane
LCP	Liquid crystal polymer
LEO	Low Earth orbit
LHe	Liquid helium

LH_2	Liquid hydrogen
LNG	Liquefied natural gas
LN_2	Liquid nitrogen
LOX	Liquid oxygen
LT	Low temperature
MWK	Multi-axial warp
PA	Polyamide
PBT	Polybutylene terephthalate
PC	Polycarbonate
PE	Polyester
PEEK	Polyetheretherketone
PEI	Polyetherimide
PES	Polyethersulfone
PI	Polyimide
PP	Polypropylene
PTFE	Polytetrafluoroethylene
PUR	Polyurethane
RLV	Reusable launch vehicles

RT	Room temperature
S_F	Flexural strength
S_T	Tensile strength
SEM	Scanning electron microscopy
T_g	Glass transition temperature
UD	Unidirectional
VE	Vinyl ester
X_C	Longitudinal compressive strength
Y_C	Transverse compressive strength
X_F	Longitudinal flexural strength
X_T	Longitudinal tensile strength
Y_T	Transverse tensile strength
Z_T	Out-of-plane tensile strength
ΔT	Temperature difference
ε	Tensile elongation at break
ε_F	Flexural elongation at break
ε_{1T}	Longitudinal tensile elongation at break
ε_{2T}	Transverse tensile elongation at break

ε_{3T}	Out-of-plane tensile elongation at break
κ	Thermal conductivity
ν	Poisson's ratio
ν_n	Poisson's ratio, $n = 12, 21, 23$ referring to planes $12, 21$ and 23
$\uparrow$	Property increase
$\downarrow$	Property decrease

1. Introduction

Fibre reinforced polymer composites are the primary material to be used in many industries, which has led to the extensive characterisation and understanding of their behaviour in ambient conditions. However, there are extremities both within and beyond the Earth's atmosphere that require structures to operate at cold (cryogenic) temperatures, where the response of the material can change significantly. Applications include liquid propellant tanks (usually composite overwrapped pressure vessels or COPVs); satellite, spacecraft and launch vehicle structures; aircraft structures at cruising altitude; support elements (struts and straps) and electrical insulation for superconducting magnets and devices operating at cryogenic temperatures; Arctic exploration structures (usually boat structures).

To design structures for these extreme applications, it is necessary to understand the effect of low and cryogenic temperatures on composite materials. This review paper

aims to cover the literature on material properties, failure mechanisms and experimental procedures, and to establish trends for future research.

Although there is not a distinct temperature point that defines the field of cryogenics, it is usually referred to as -150 °C, below which the boiling points of oxygen, nitrogen, hydrogen and helium occur. The upper limit of the so-called “high-temperature” cryogenics is at -50 °C, which is also chosen for the upper temperature to be addressed in this work. This paper refers to the -273 °C (0 K) to -150 °C (123 K) range as cryogenic temperature (CT), the -150 °C (123 K) to -50 °C (223 K) range as low temperature (LT) and approximately 23 °C as room temperature (RT). Nominal temperatures of interest can be seen in Table 1.

Table 1. Temperatures of interest for the investigation of cryogenic and low temperature composites

Description	[K]	[°C]	Category
Room temperature	296	23	RT
Design temperature for Arctic conditions	223	-50	LT
Design temperature for aircraft components	216	-57	LT
Solid carbon dioxide (dry ice)	195	-78	LT
Design temperature for cubesats	188	-85	LT
Lowest temperature measured on Earth	184	-89	LT
Liquid methane (LCH_4) or natural gas (LNG)	111	-162	CT
Lowest temperature in low Earth orbit (LEO)	103	-170	CT
Liquid oxygen (LOX)	90	-183	CT
Liquid nitrogen (LN_2)	77	-196	CT
Liquid hydrogen (LH_2)	20	-253	CT
Liquid helium (LHe)	4.2	-269	CT
Temperature in empty space	3	-270	CT
Absolute zero	0	-273	CT

This work focuses on the literature published since 1994, the year of the latest comprehensive review article written in this field by Reed and Golda [1], accounting for the literature between 1980 and 1994. Newer review articles have been published by Schultz [2], Aoki et al. [3], Fu et al. [4], Horiuchi et al. [5], Sethi et al. [6], Li et al. [7], Yano et al. [8] and Bay et al. [9], but they have limited coverage of the literature or address only indirectly related topics. For the sake of completeness, the reader can

refer to older review articles covering the periods of 1975-1981 [10] and 1960-1975 [11–13] and reviews on cryogenic strap and strut structures [14,15].

2. Material properties

2.1. Modulus, strain and strength

2.1.1. Tension

The Young's modulus and tensile strength of the matrix tend to increase with decreasing temperature.

The reason for this is the reduction in polymer chain mobility, which increases the binding forces between the molecules, and therefore the strength of the material. Furthermore, according to the principle of time-temperature superposition, the lower the temperature, the more time it takes for stresses to relax. At cryogenic temperatures the relaxation can be completely arrested, resulting in increased stiffness [16–21]. See Table 2 for the summary of the effects of low and cryogenic temperatures on the material properties of resins.

Table 2. Summary of the effect of low and cryogenic temperatures on resin material properties

Resin	T [K]	Property change compared to RT	Ref.
Thermoset resin			
Epoxy (CYD-128)	77	E↑72%, S_T↑26%, ε↓33%	[18]
Epoxy (DGEBA)	4	E↑172%, ν↑52%	[22]
Epoxy (DGEBA)	77	E↑112%, ν↑38%	[22]
Epoxy (DGEBF)	93	E↑133%	[23]
Epoxy (DGEBF)	90	E↑206%, S_T↑66%, ε↓64%	[24]
Epoxy (DGEBF)	77	S_T↑, ε↓	[25]
Epoxy (DGEBF)	77	E↑42%	[26]
Epoxy (DGEBF)	77	E↑37%, S_T↑19%, ε↓35%	[27]

Epoxy (DGEBF)	77	E↑72%, S_T↑26%, ε↓46%	[20]
Epoxy (R608)	77	E↑34%, E_F↑126%, S_F↑65%, S_T↓24%, ε↓62%	[28]
Epoxy (WSR615)	77	E↑, S_T↑	[29]
Epoxy (YD-128)	77	E↑73%, S_T↑19%, ε↓	[30]
Epoxy (YD-128)	77	E↑79%, S_T↑25%, ε↓	[31]
Epoxy (828)	153	E↑136%, S_T↓, ε↓	[32]
DCPD	77	E↑, S_T↑, ε↓	[33]
Thermoplastic resin			
PEEK	4	E↑100%	[34]
PEEK	77	E↑74%	[34]
PES	77	E↑, E_F↑, S_F↑, S_T↑, ε↓, ε_F↓	[17]
PES	77	E↑62%	[35]
PA12	77	E↑224%	[35]
PC	77	E↑91%, S_T↑140%, ε↓	[36]
PI (PETI-5)	84	E↑150%, S_T↑98%, ε↓83%	[37]
PI (8515)	84	E↑97%, S_T↑11%, ε↓53%	[37]
PI (5050)	85	E↑104%, S_T↑34%, ε↓69%	[37]
Thermoset/thermoplastic resin			
LCP (LCR)	84	E↑143%, S_T↓29%, ε↓78%	[37]

The behaviour of single carbon fibres at CT was explored by Zhang et al. [38]. Unlike polymers, the molecular structure of fibres is not homogeneous, and due to the high-temperature heat treatment applied during manufacturing, the level of their crystallinity and molecular orientation is already near optimal. Thus, further improvement cannot be practically achieved by exposing them to cryogenic temperatures and their modulus increases only marginally [39]. Due to the cracking of the carbon fibre (CF) surface at CT (see Section 2.5 for description), the single fibre strength decreases with decreasing temperature. Kevlar fibres (or aramid fibres, AF), however, possess different molecular structure and increased strength can be achieved with cryogenic treatment [40].

However, the effect of reduced carbon fibre strength is overshadowed by the effect of the increased fibre-resin interface strength at CT, which is related to the thermal expansion of the constituents and is discussed in depth in Section 2.5. Subsequently,

the longitudinal Young's modulus and tensile strength of the composite also increases with decreasing temperature. As the transverse strength and stiffness properties are dominated by the resin and fibre-resin interface, transverse property improvement at CT is also evident for fibre-reinforced composites. Only a marginal portion of the literature mentions decreased longitudinal composite strength: [41,42] for UD epoxy, [43] for woven epoxy and [44–46] for UD thermoplastic composites. A possible explanation can be the internal stresses present in the laminate due to the thermal expansion of the fibre and resin during cooldown from cure temperature to RT, then to cryogenic temperatures. The thermal expansion phenomenon is addressed in Section 2.5. See Table 3 for the summary of the effects of low and cryogenic temperatures on the tensile material properties of composites.

Table 3. Summary of the effect of low and cryogenic temperatures on the tensile properties of composites. In those cases, where several types of material structures were investigated, only the most beneficial content is cited

Resin	Fibre	Structure	T [K]	Property change compared to RT	Ref.
Thermoset resin – Carbon fibre					
Epoxy (CU-125 NS)	CF (T700)	UD	123	E_{1T}↑16%, X_T↓9%	[41]
Epoxy (DGEBA)	CF	UD	123	E_{2T}↑, Y_T↑	[47]
Epoxy (DGEAC)	CF (T700)	UD	77	X_T↑, Y_T↑	[48]
Epoxy (DGEAC)	CF (T800)	UD	77	X_T↑, Y_T↑	[48]
Epoxy (DGEBF)	CF (T700)	UD	93	E_{1T}=, E_{2T}↑49%	[23]
Epoxy (E618)	CF (TC-33)	UD	77	E_{1T}↑, X_T↑20%, ε_{1T}↑	[49]
Epoxy (RIM135)	CF (T300)	3D MWK (Type A)	77	E_F↑50%, E_{1T}↑47%, X_F↑81%, X_T↑58%, ε_{1T}↑8%	[50]
Epoxy (R118)	CF (T300)	Woven	77	E_F↓11%, X_F↓8%	[51]

Epoxy (R118)+GO	CF (T300)	Woven	77	E_F↓2%, X_F↓1%	[51]
Epoxy (R608)	CF (M40)	UD	77	X_F↑, X_T↑	[28]
Epoxy (828)	CF (HM50)	UD	77	E_{1T}↑36%, X_T↓10%, ε_{1T}↓53%	[42]
Epoxy (862)	CF	Woven	77	E_F↓4%, E_{1T}=, X_F↓4%, X_T↓3%	[52]
Epoxy (977-2)	CF (IM7)	UD	77	E_{2T}↑37%, Y_T↑12%	[53]
Epoxy (977-3)	CF (IM7)	UD	77	E_{2T}↑21%, Y_T↑29%	[54]
Epoxy (3633)	CF (T800H)	Woven	4	E_{1T}↑8%, E_{2T}↓2%, ν_{12}↑49%	[55]
Epoxy (3633)	CF (T800H)	Woven	4	X_T↓15%	[43]
Epoxy (3633)	CF (T800H)	Woven	77	X_T↓5%, Y_T↓20%	[43]
VE	CF	UD	173	E_F↑, X_F↑55%, ε_F↑	[56]
Thermoset resin – Glass fibre					
Epoxy	GF (E-glass)	3D MWK (Type D)	77	E_{1T}↑83%, X_T↑104%, ε_{1T}↑	[57]
Epoxy (DGEBA)	GF (G-11)	Woven	77	E_{3T}↑75% (Type A specimen), Z_T↑80% (Type B specimen), ε_{3T}↓	[58]
Epoxy (DGEBA)	GF (SL-ES30)	Woven	77	E_F↑25%, E_{1T}↑31%, E_{2T}↑14%, X_F↑94%, X_T↑94%, ν_{12}↑36%	[59]
Epoxy (E51)	GF (E-glass)	UD	77	E_{1T}↑, X_T↑30%, ε_{1T}↑	[49]
Epoxy (EL-762H)	GF (G-11)	Woven	4	E_{1T}↑28%, X_T↑94%, ν_{12}↑33%	[60]
Epoxy (EL-762H)	GF (G-11)	Woven	20	E_{1T}↑27%, X_T↑92%, ν_{12}↑28%	[60]
Epoxy (EL-762H)	GF (G-11)	Woven	77	E_{1T}↑22%, X_T↑91%, ν_{12}↑28%	[60]
Epoxy (ML-506)	GF	UD	213	E_{1T}↑24%, E_{2T}↑, X_T↑12%, Y_T↑, ε_{1T}↓14%, ε_{2T}↓	[61]
Epoxy (RIM135)	GF (E-glass)	3D MWK (various types)	77	E_F↑100% (type A), X_F↑89% (type A), ε_F↑ (types B and C)	[62]
Thermoset resin – Other fibre					
Epoxy	PE	Nonwoven	77	E_F↑96%, E_{1T}↑80%, X_F↑63%, X_T↑55%, ε_F↓, ε_{1T}↓25%	[63]
Epoxy (828)	AF	UD	77	E_{1T}↑33%, X_T↓13%, ε_{1T}↓52%	[42]
Epoxy (862)	AF	Woven	77	E_F↓1%, E_{1T}↓5%, X_F↓2%, X_T↓2%	[52]
Epoxy (1266)	Zylon	UD	77	E_{1T}↑8%, X_T↑30%	[64]
Thermoplastic resin – Carbon fibre					
BMI (QY9611)	CF (ZT7H)	UD	153	E_{1T}↓5%, E_{2T}↑24%, X_T↓24%, Y_T↓31%, ε_{1T}↓, ε_{2T}↓	[44]
BMI (QY9611)	CF (ZT7H)	UD	153	E_{2T}↑24%, X_T↓18%, ε_{2T}↓, ν_{21}↑52%	[45]
BMI (5250-4)	CF (IM7)	UD	77	E_{2T}↑9%, Y_T↑12%	[53]
BMI (5250-4)	CF (IM7)	UD	77	E_{1T}↑1%, E_{2T}↑15%, ν_{12}=, ν_{23}=	[65]

PEEK	CF (AS4)	UD	4	E_{1T}↑11%, E_{2T}↑41%	[34]
PEEK	CF (AS4)	UD	77	E_{1T}↑10%, E_{2T}↑34%	[34]
PES	CF (C30 S003/6 APS)	Short fibre	77	E_F↑, E_{1T}↑, X_F↑, X_T↑, ε_F↑, ε_{1T}↑	[17]
PI (AFR-PE-4)	CF (T650)	UD	77	Y_T↑	[66]
PI (PETI-5)	CF (IM7)	UD	4	E_{1T}↓8%, E_{2T}↓10%, X_T↓22%, Y_T↓77%	[46]
PI (PETI-5)	CF (IM7)	UD	77	E_{1T}↓4%, E_{2T}↓14%, X_T↓16%, Y_T↑23%	[46]
Thermoplastic resin – Glass fibre					
PEEK	GF	Chopped fibre	20	E_F↑14%, E_{1T}↑57%, X_F↓15%, X_T↑44%, ε_{1T}↓20%	[19]
PEEK	GF	Chopped fibre	77	E_F↑7%, E_{1T}↑35%, X_F↓7%, X_T↑38%, ε_{1T}↓13%	[19]
Thermoplastic resin – Other fibre					
PP	PP	Woven	77	E_F↑114%, X_F↑34%, ε_F↓50%	[67]

As the resin loses its ductility and increases its stiffness at CT, the elongation at break and fracture toughness (see section 2.3) decrease at the same time. The same effect occurs with single carbon fibres [39], whereas glass fibres (GF) experienced increased elongation at break [68]. The latter case was explained by the author as a structural level phenomenon: cracks accumulate at CT but cannot extend to trigger complete material failure, instead their density increases, which acts as a stress relief and enables larger elongation. The creep of Kevlar fibres was measured by Bersani et al. and the material showed excellent response at 4.2 K [69].

The fracture of carbon fibre/bismaleimide unidirectional laminates in tension can be seen in Fig. 1. The specimen tested at -120 °C shows a clear fracture plane perpendicular to loading direction (Fig. 1a). The RT specimen (Fig. 1b) is shattered into several chunks due to its ductility and subsequent redistribution of load after local fibre failures.

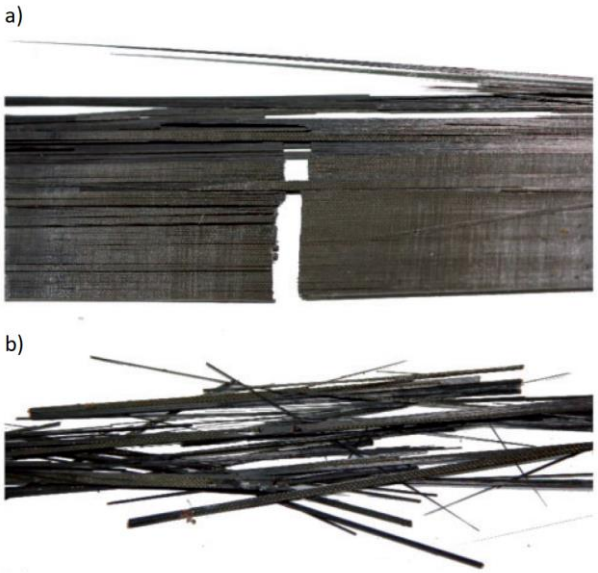

Fig. 1. Fracture of carbon fibre/bismaleimide unidirectional laminates in tension: a) at -120 °C b) at RT (Reproduced by permission of the copyright holder from [44]. Selected images are cropped from the original figure.)

Poisson's ratio should become lower with decreasing temperature due to the increased stiffness of the resin [70], but several authors reported increased values at CT [45,55,59,60]. A possible explanation can be the difference in increase in longitudinal (E_1) and transverse (E_2) elastic modulus. If E_1 is more sensitive to decreasing temperature, then the relative difference between E_1 and E_2 will increase too, thus the longitudinal Poisson's ratio becomes higher.

2.1.2. Compression

Similarly to tension, the molecular behaviour of the resin at CT is reflected in the compressive properties: the compressive modulus and strength of the resin increase and the failure strain decrease with decreasing temperature [71,72].

Kevlar fibres have a fibrillar microstructure, anisotropic thermal contraction and low adhesion to the matrix (see Section 2.5), which leads to low compressive strength. Boron fibres have large diameter, which leads to increased compressive strength (based on composite properties [2]). Whereas these properties are true for RT conditions, it is important to point out the applicability of Kevlar fibres, as they can be the optimal or avoidable choice for tension and compression in cold temperatures, respectively.

As the matrix is responsible for supporting the fibres when subjected to compressive loading, its increased stiffness and the increased fibre-resin interfacial strength provide increased longitudinal compressive strength and stiffness for composite materials. The improved support also shifts the failure from kinking to fracture at lower temperatures [61,73–75]. Table 4 summarises the effects of low and cryogenic temperatures on the compressive material properties of composites.

Table 4. Summary of the effect of low and cryogenic temperatures on compressive properties of composites. In those cases, where several types of material structures were investigated, only the most beneficial content is cited

Resin	Fibre	Structure	T [K]	Property change compared to RT	Ref.
Thermoset resin – Carbon fibre					
Epoxy	CF (T700)	UD	213	E_{1C}=, X_C↑21%	[74]
Epoxy (JC-02A)	CF (T700)	Braided (26°)	173	E_{1C}↑, X_C↑	[76]
Epoxy (RIM135)	CF (T300)	3D MWK (various types)	77	E_{1C}↑50%, E_{2C}↓26%, X_C↑27%, Y_C↑73%	[77]
Epoxy (R608)	CF (M40)	UD	77	X_C↑	[28]
Epoxy (DGEAC)	CF (T700)	UD	77	X_C↑, Y_C↑	[48]

Epoxy (DGEAC)	CF (T800)	UD	77	X_C↑, Y_C↑	[48]
Thermoset resin – Glass fibre					
Epoxy	GF (E-glass)	UD	213	E_{1C}↑15%, X_C↑10%	[73]
Epoxy (ML-506)	GF	UD	213	E_{1C}↑, E_{2C}↓, X_C↑28%, Y_C↑52%	[61]
Epoxy (TDE-86)	GF (E-glass)	Braided (20°)	77	E_{1C}↑15%, E_{2C}↑42%, X_C↑52%, Y_C↑96%	[78]
Epoxy (DGEBA)	GF (SL-ES30)	Woven	77	X_C↑142%, Y_C↑117%	[79]
Thermoset resin – Other fibre					
Epoxy	PE	Nonwoven	77	E_{1C}↑94%	[63]
Thermoplastic resin					
BMI (QY9611)	CF (ZT7H)	UD	153	E_{1C}↑1%, E_{2C}↑7%, X_C↑13%, Y_C↑23%	[44]
PI (PETI-5)	CF (IM7)	UD	4	E_{1C}↑9%, E_{2C}↑10%, X_C↑39%, Y_C↑67%	[46]
PI (PETI-5)	CF (IM7)	UD	77	E_{1C}↑5%, E_{2C}↑3%, X_C↑31%, Y_C↑34%	[46]

Specimens subjected to three-point bending loading case also show improvement at CT, but as one side of the coupon is in tension and the other is in compression, the failure mechanism can change with decreasing temperature [56,62,80]. In one case, with unidirectional (UD) carbon fibre reinforced polymer (CFRP) composites, the kinking failure of the compression (top) face of the specimens transitioned into a crack failure at -60 °C and remained intact at -100 °C [56]. In another case, with woven glass fibre reinforced polymer (GFRP), the damage area became larger and multiple cracks appeared, or the intact surface became damaged at 196 °C [62].

There is a rising interest in the literature about the cryogenic behaviour of braided composites. Not only do these structures have enhanced compressive properties at lower temperatures, but they can be tailored to have near-zero coefficient of thermal expansion (CTE) by the optimisation of the braid angle [76,78,81–84].

Pinned specimens delivered higher ultimate compressive and bearing strength [85] and higher yield strength [86] at low temperatures. (Note that the compression after impact (CAI) strength is addressed in Section 2.4.)

2.1.3. Shear

The shear behaviour of fibre-reinforced composites is primarily controlled by the behaviour of the matrix. As described above, in tension, the resin becomes more rigid, stronger, and its failure strain decreases at cold temperatures. When subjected to shear loading, these effects are also accompanied by the elimination of the nonlinearity in the shear stress – shear strain response with decreasing temperature [43]. This can be described by observing the scanning electron microscopy (SEM) images of the fractures surface of failed short-beam shear specimens (Fig. 2). The fracture surface consists of river patterns converging in the direction of the crack growth. At RT (Fig. 2b), these cusps are deeper and undergo larger deformation due to yielding, but at -100 °C (Fig. 2a) their size is smaller and their density is higher. This indicates sudden fracture upon specimen failure, and subsequent linear response in the stress – shear strain curve.

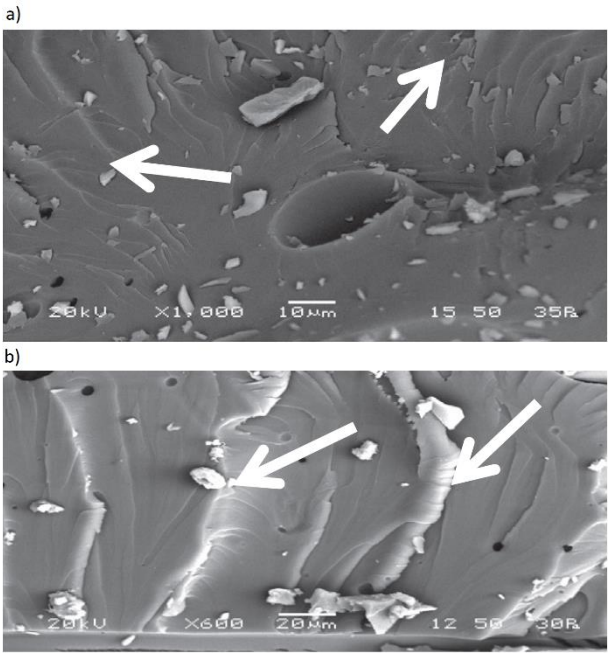

Fig. 2. SEM images of shear cracking in glass fibre/epoxy composites: a) at -100 °C b) at RT (Reproduced by permission of the copyright holder from [87]. Selected images are cropped from the original figure. Arrows are unrelated to the context in this paper.)

The secondary driving factor of shear strength is the fibre-resin interface. Woven Kevlar fibres demonstrated lower interlaminar shear strength (ILSS) than carbon fibres with the same resin at -196 °C [52] and in at other study at -100 °C [87]. This can be explained by the poor interfacial properties between Kevlar fibres and resins [87]. In the latter study, composites with glass fibre showed higher ILSS than with carbon fibres. However, the CFRP laminates did not show any improvement at LT compared to RT, which is contrary to the literature, as ILSS generally increases with decreasing temperature.

Only a few investigations from Bay's research group reported decreasing ILSS at cold temperatures [88–90], whereas Yang et al. reported reduction in in-plane shear

strength (IPSS) with bismaleimide (BMI) resin specimens at -120 °C [44]. Narita's research group revealed lower ILSS at 20 K compared to RT [91], however, they also measured lower values at 4 K compared to 77 K (without RT comparison) in another work [92]. As most works do not cover temperatures below 77 K, based on the two works above, it is possible that the ILSS first increases with decreasing temperature, then decreases as the temperature approaches near-zero K. Again, a contributing factor can be the internal stresses in the laminate due to thermal expansion (see Section 2.5). It is possible that below 77 K these internal stresses become more critical than the stresses present in the material because of the mechanical loading. See Table 5 for a summary of the effects of low and cryogenic temperatures on the shear material properties of composites.

Table 5. Summary of the effect of low and cryogenic temperatures on shear properties of composites

Resin	Fibre	Structure	T [K]	Property change compared to RT	Ref.
Thermoset resin					
Epoxy (DGEBA)	CF	Woven	173	ILSS↑3%	[87]
Epoxy (DGEBA)	GF	Woven	173	ILSS↑86%	[87]
Epoxy (DGEBA)	AF	Woven	173	ILSS↓32%	[87]
Epoxy (DGEBA)	GF (G-10)	Woven	77	ILSS↑29%-85% (depending on specimen geometry)	[93]
Epoxy (DGEBA)	GF (E-glass)	Woven	77	ILSS↓26%	[89]
Epoxy (DGEBA)	GF (E-glass)	Woven	213	ILSS↓15%	[89]
Epoxy (DGEBA)	GF (G-10CR)	Woven	4	ILSS↑113%-180% (depending on specimen geometry)	[94]
Epoxy (DGEBA)	GF (G-10CR)	Woven	77	ILSS↑97%-156% (depending on specimen geometry)	[94]
Epoxy (DGEBA)	CF (T700)	UD	123	IPSS↑	[47]
Epoxy (ML-506)	GF	UD	213	G_{12}↑, ILSS↑	[61]

Epoxy (R608)	CF (M40)	UD	77	ILSS↑	[28]
Epoxy (WSR615)	GF	Woven	77	ILSS ↑	[95]
Epoxy (862)	CF	Woven	77	ILSS=	[52]
Epoxy (862)	AF	Woven	77	ILSS↓17%	[52]
Epoxy (913)	GF (E-glass)	Woven	223	ILSS↑	[96]
Epoxy (977-2)	CF (T700)	UD	77	G_{12}↑37%, IPSS↑10%	[53]
Epoxy (977-3)	CF (T700)	UD	77	G_{12}↑51%, IPSS↑17%	[54]
Epoxy (3633)	CF (T800H)	Woven	4	G_{12}↑139%	[55]
Epoxy (3633)	CF (T800H)	Woven	20	ILSS↓19%	[91]
Thermoplastic resin					
BMI (QY9611)	CF (ZT7H)	UD	153	G_{12}↑39%, IPSS↓29%	[44]
BMI (5250-4)	CF (IM7)	UD	77	G_{12}↑64%	[65]
BMI (5250-4)	CF (T700)	UD	77	G_{12}↑65%, IPSS ↑23%	[53]
PI (PETI-5)	CF (IM7)	UD	4	G_{12}↑35%	[46]
PI (PETI-5)	CF (IM7)	UD	77	G_{12}↑26%	[46]

2.2. Fatigue

The fatigue of composites is driven by matrix crack initiation and accumulation. This cannot only occur because of pure mechanical loading, but at cryogenic temperatures, the excessive thermal expansion and subsequent thermal stresses can also fracture the brittle resin. Thermal cycling is a critical load case for: reusable launch vehicles (RLV) going to and returning from space, spacecraft and satellites operating in the shadow of Earth and in direct sunlight, and for COPVs due to repeated refuelling. To prevent matrix cracking, there are strict strain allowables in place (e.g. 0.5% tensile and 0.33% compressive for COPVs [97]), but these can lead to overweight structures. Hence,

there is a need to understand the fatigue of composites at cold temperatures to enable the design of fatigue-resistant components.

2.2.1. Mechanical fatigue

The mechanical fatigue strength of composites at lower temperatures is generally better than at room temperature [1,2,22,42,93,98–112]. To the authors' best knowledge, the only exceptions in the literature are two studies carried out on the same CFRP specimens under mode I loading, where it was found that the crack propagation length was higher at -60 °C than at RT [113,114]. The fatigue performance increases with increasing fibre tensile modulus, and the rate of change is higher at 77 K than at RT according to [1,15], but the effect of fibre material was not assessed and could possibly be responsible for the difference. It was also found that going down from 77 K to 4.2 K the rate of crack propagation increases, possibly due to the decreased fracture toughness of the resin [98–100,103]. Moreover, there is a difference in matrix type, as toughened epoxy and thermoplastic resins provide higher fatigue resistance than brittles ones [2,113]. Based on open hole tensile fatigue tests, the fatigue life increases with decreasing temperature. However, if the load rate is increased, the opposite behaviour can occur: the fatigue life decreases with decreasing temperature [115].

The reason for the improved fatigue performance with decreasing temperature is the increased resin strength (see Section 2.1) and the increased fibre-resin interface strength (see Section 2.5) [22,109]. The latter can be observed in Fig. 3, where the fracture surfaces of woven glass fibre reinforced polymer specimens subjected to

mode I cyclic loading can be seen. At RT (Fig. 3a), the fibre surfaces are almost entirely free of resin debris, which indicates the low interfacial strength. By decreasing the temperature to 77 K (Fig. 3b), the fibres remain covered in resin, indicating improved interfacial strength.

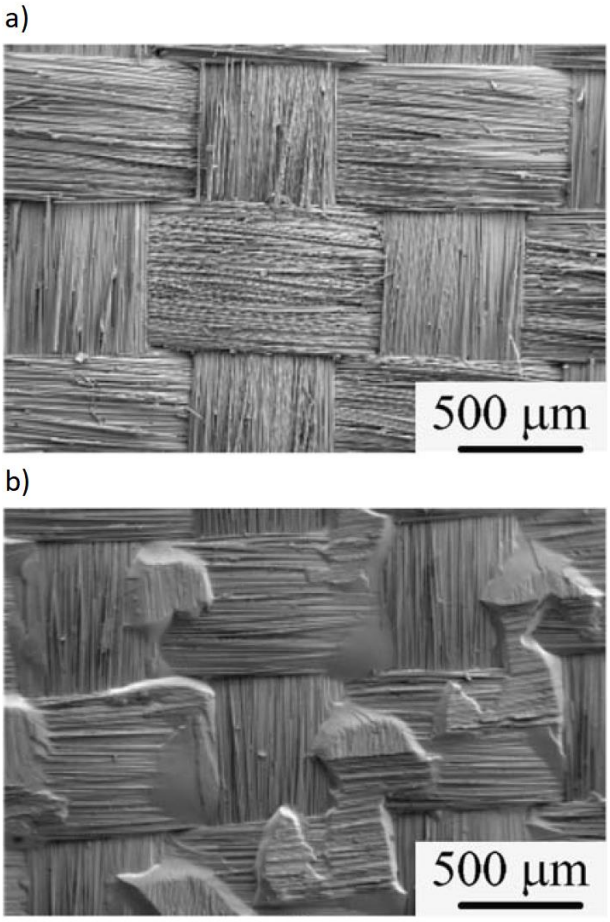

Fig. 3. SEM micrographs of typical fracture surfaces of GFRP woven laminates associated with mode I cyclic fatigue: a) at RT b) at 77 K (Reproduced by permission of the copyright holder from [109]. Selected images are cropped from the original figure.)

2.2.2. Thermal fatigue

Mechanical fatigue tests are usually carried out purely for strength and stiffness evaluation, but thermal fatigue investigations also include permeability (see Section 2.8), outgassing and vacuum [116–121] effects. Cycle times of interest can range from 10^1 to 10^2 (e.g. refuelling of COPVs of RLVs) and up to 10^4-10^5 (e.g. satellite service life). To the authors' best knowledge, there is no investigation in the literature above 10^4 (10^4 is examined in [122]) due to the complexity of thermal cycling experiments.

There are two main types of thermal cycling: from RT to CT and from high temperatures (HT) to CT. The former is a typical load case for insulated COPVs in launch vehicles, which are protected from the heat of sunlight and re-entry, whereas the latter is typical for satellite structures alternating between sunlight and the shadow of the Earth. A HT-CT cycle not only means the resin must be operational at HT, but the temperature difference (ΔT) and therefore thermal expansion is higher too.

Cracks can occur even after the first cycle[123,124], and even if their density remains the same after subsequent cycles, the crack lengths can increase and contribute to higher permeability or lower material properties [124,125]. The number of cracks as a function of thermal cycles depends on several parameters. Subjected to higher ΔT [126–129] and higher cooling rate [130,131], composites develop more cracks under the same number of cycles. Laminates with tougher resins [53,122,132,133], resins with lower CTE [132], fibres with lower CTE [132], fibres with lower modulus [132], fibres with sizing [134] and laminates with lower porosity [124] are more resistant to

crack development. Smoother surface roughness on the specimen [132] and lower laminate thickness due to smaller thermal stress gradient through-the-thickness [123] leads to fewer cracks. The crack formulation also depends on the layup [46,53,54,123,135–139] (Fig. 4).

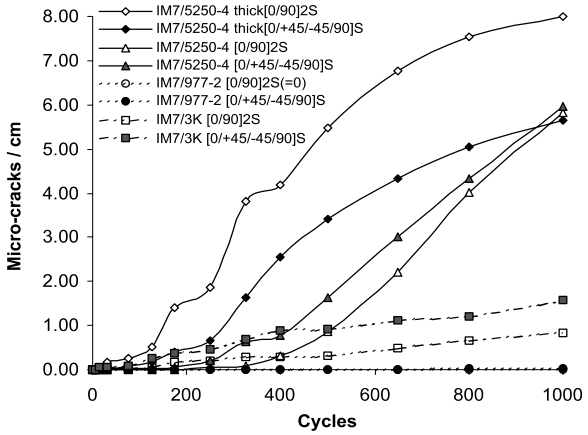

Fig. 4. Microcrack density in surface plies of laminates with different material and stacking sequence subjected to thermal cycling between RT and -196 °C (Reproduced by permission of the copyright holder from [53])

Several authors reported first increasing, then decreasing, then plateauing mechanical properties with increasing number of cycles [41,117,119]. The reason for the increase is the higher resin strength and stiffness at CT. This is followed by the decrease of properties, because of the accumulation of cracks and subsequent loss of strength overthrows the positive effect of CT on the material. Finally, the plateau is present because the matrix cracks relieve the stress concentrations in the material [119]. Other authors experienced first decreasing, then increasing, then plateauing properties [116,117,140]; constantly decreasing properties [117,135,141–144], constantly increasing [47], and unchanged properties [135,145,146].

There is a comprehensive coverage of thermal cycling in the literature and the correlation between the aforementioned parameters and the crack density as function of thermal cycles is well understood. However, the correlation between mechanical properties and crack density as function of cycles is unclear and needs further research.

2.3. Fracture toughness

Fracture toughness defines the damage tolerance of materials as their ability to resist crack propagation. Usually fracture toughness (K_C) of the pure resin and critical strain energy release rate (G_C) of the laminated composite material (interlaminar fracture toughnness) are measured. As G_C is function of K_C, both properties are referred to as fracture toughness in this work, and are only distinguished by their symbols. However, G_C is also inversely proportional to the elastic moduli of the material (Young's modulus for mode I and shear modulus for mode II), which are temperature dependent (increase with lowering temperature, see Section 2.1). Therefore a case can exist where the K_C of the resin is higher at CT than RT, but G_C of the composite material using the same resin is lower at CT. Hence, the G_C characterisation of the composite material is necessary and material selection for cryogenic application shall not be based merely on the improved K_C of the resin at CT.

A number of studies have shown increased K_{IC} of pure epoxy at 77 K [27,37,147] or 90 K [24] or 123 K [148] compared to RT, whereas one work presented a lower value at 153 K [32] (see Table 6). The improved fracture toughness of a polymer is related to the molecular movement at cryogenic temperatures. As the chain mobility reduces,

the binding intermolecular forces between them increase (see section 2.1.1). This increases the fracture toughness. On the one hand, the "free volume" between the molecules almost disappears at cold temperatures, which supresses the stress relaxation at the crack tip, and leads to decreased fracture toughness. On the other hand, the "free space" within the molecules still exist, which alleviates the effect of the lack of free volume, and makes the stress relaxation possible, but much more limited as compared to RT (Fig. 5) [149]. Depending on the molecular structure of an epoxy, the available free space can differ at lower temperatures and may or may not be able to generate fracture toughness improvement. At near-zero temperatures, the molecular movement of the epoxy is frozen, which restricts the stress relaxation and leads to decrease in fracture toughness [149].

Table 6. Summary of the effect of low and cryogenic temperatures on fracture toughness of resins

Resin	T [K]	Property change compared to RT	Ref.
Thermoset resin			
Epoxy (DGEBF)	90	K_{IC}↑43%	[24]
Epoxy (YD-114F)	123	K_{IC}↑130%	[148]
Epoxy (YD-128)	77	K_{IC}↑71%	[147]
Epoxy (828)	153	K_{IC}↓19%	[32]
Thermoplastic resin			
PI (PETI-5)	79	K_{IC}↑63%	[37]
PI (8515)	83	K_{IC}↑23%	[37]
PI (5050)	84	K_{IC}↑45%	[37]
LCP (LCR)	84	K_{IC}↑26%	[37]

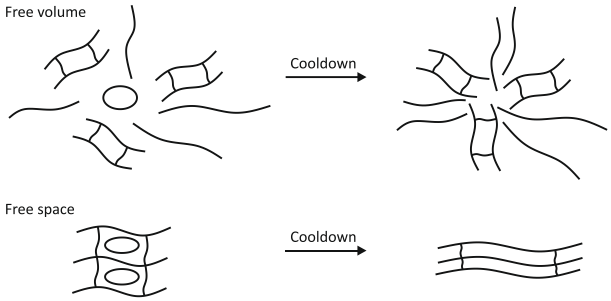

Fig. 5. Schematic illustration of free volume and free space (Reproduced by permission of the copyright holder from [149]. Original figure redrawn.)

Similar behaviour should occur with laminated composites, as the fracture is also dominated by the resin. However, among all the investigated composites in the literature, only half of the resins (CU125NS, DGEBA, SE-84, 133) showed increased properties and the other half (977-2, 977-3, 3501-6, 3631) showed decreased properties at cryogenic or low temperatures (see Table 7). This distinction is independent of fibre type (carbon or glass), ply type (UD or woven), and resin generation (untoughened “Generation 1” or toughened “Generation 2”). A possible explanation can be the discrepancies in experimental methods across the literature (see Section 3), which in enhanced by the sensitivity of fracture toughness measurement.

Studies not included in Table 7 reported non-interlaminar fracture toughness measured by single-edge-notched bend [150] and tensile compact tension [151,152] specimens; fatigue behaviour [22,102,108]; and fracture toughness of adhesively bonded joints [153,154].

Table 7. Summary of the effect of low and cryogenic temperatures on fracture toughness of composites

Resin	Fibre	Structure	T [K]	Property change compared to RT	Ref.
Thermoset resin					
Epoxy (CU125NS)	CF (T700)	UD	123	G_{IC}↑	[155]
Epoxy (DGEBA)	CF (T700)	UD	77	G_{IIC}↑	[156]
Epoxy (DGEBA)	Alumina	UD	77	G_{IC}↑80%, G_{IIC}↑80%	[157]
Epoxy (DGEBA)	GF (G11)	Woven	4	G_{IIC}↑159%	[158]
Epoxy (DGEBA)	GF (G11)	Woven	77	G_{IIC}↑144%	[158]
Epoxy (DGEBA)	GF (G11)	Woven	4	G_{IIIC}↑42%	[159]
Epoxy (DGEBA)	GF (G11)	Woven	20	G_{IIIC}↑57%	[159]
Epoxy (DGEBA)	GF (G11)	Woven	77	G_{IIIC}↑48%	[159]
Epoxy (DGEBA)	GF (G11)	Woven	4	G_{TC}↑60% (G_{II}/(G_I+G_{II})=0.76)	[160]
Epoxy (DGEBA)	GF (G11)	Woven	77	G_{TC}↑56% (G_{II}/(G_I+G_{II})=0.76)	[160]
Epoxy (DGEBA)	GF (G11)	Woven	4	G_{TC}↓10% (G_{III}/(G_I+G_{III})=0.77)	[161]
Epoxy (DGEBA)	GF (G11)	Woven	77	G_{TC}↑20% (G_{III}/(G_I+G_{III})=0.78)	[161]
Epoxy (DGEBA)	GF (G11)	Woven	4	G_{TC}↑6% (G_{III}/(G_{II}+G_{III})=0.75)	[162]
Epoxy (DGEBA)	GF (G11)	Woven	77	G_{TC}↑15% (G_{III}/(G_{II}+G_{III})=0.74)	[162]
Epoxy (DGEBA)	GF (SL-E)	Woven	4	G_{IC}↓13%	[163]
Epoxy (DGEBA)	GF (SL-E)	Woven	77	G_{IC}↑21%	[163]
Epoxy (DGEBA)	GF (SL-E)	Woven	4	G_{IIC}↑96%	[164]
Epoxy (DGEBA)	GF (SL-E)	Woven	77	G_{IIC}↑118%	[164]
Epoxy (DGEBA)	GF (SL-EC)	Woven	4	G_{IC}↓14%	[165]
Epoxy (DGEBA)	GF (SL-EC)	Woven	77	G_{IC}↑49%	[165]
Epoxy (DGEBA)	GF (SL-EC)	Woven	4	G_{IC}↓8%, G_{IIC}↑90%, G_{TC}↑89% (G_{II}/(G_I+G_{II})=0.59)	[166]
Epoxy (DGEBA)	GF (SL-EC)	Woven	77	G_{IC}↑56%, G_{IIC}↑80%, G_{TC}↑38% (G_{II}/(G_I+G_{II})=0.59)	[166]
Epoxy (SE-84)	CF	Woven	77	G_{IC}↑96%	[167]
Epoxy (133)	CF (IM600)	UD	4	G_{IC}↑	[168]
Epoxy (133)	CF (IM600)	UD	77	G_{IC}↑	[168]
Epoxy (977-2)	CF (IM7)	UD	77	K_{IC}↓1% (notched four point bending specimen)	[169]
Epoxy (977-2)	CF (IM7)	UD	77	G_{IC}↓	[170]
Epoxy (977-2)	CF (T700)	UD	77	G_{IIC}↓5%	[53]
Epoxy (977-3)	CF (T700)	UD	77	G_{IIC}↓35%	[54]
Epoxy (3501-6)	CF (AS4)	UD	213	G_{IC}↓15%	[114]
Epoxy (3631)	CF (T800)	UD	77	G_{IC}↓27%	[167]
Thermoplastic resin					
BMI (5250-4)	CF (T700)	UD	77	G_{IIC}↓5%	[53]
PI (PETI-5)	CF (IM7)	UD	77	G_{IC}↑	[170]

2.4. Impact

In most cases the impact behaviour of composite structures is studied to address low velocity impact of foreign objects (e.g. bird strike on aircraft), assembly and maintenance accidents (e.g. tool drop), and slam loading of ship hulls. In the field of cryogenic composites, two additional aspects need to be considered: high-velocity and hypervelocity impact due to space debris in orbit [171–176] and the flammability of propellants in COPVs due to ignition following an impact event [177–180].

The general trend according to literature is decreasing resin impact performance with decreasing temperature (see Table 8). The reason for this is the reduced resin ductility at cryogenic temperatures. This prevents the matrix from yielding and leads to lower energy required to break the sample [20] (Fig. 6).

Table 8. Summary of the effect of low and cryogenic temperatures on impact behaviour of resins

Resin	T [K]	Property change compared to RT	Ref.
Thermoset resin			
Epoxy (CYD-128)	77	$I\downarrow$2%	[18]
Epoxy (DGEBF)	77	$I\downarrow$37%	[20]
Epoxy (DGEBF)	77	$I\downarrow$	[25]
Epoxy (R608)	77	$I\downarrow$12%	[28]
Epoxy (WSR615)	77	$I\downarrow$15%	[29]
Epoxy (YD-128)	77	$I\downarrow$33%	[16]
Epoxy (YD-128)	77	$I\downarrow$51%	[181]
Epoxy (YD-128)	77	$I\downarrow$28%	[31]
Thermoplastic resin			
PEEK	198	$E_{abs}\downarrow$	[182]
PP (HP500 M)	77	$I\downarrow$21%	[183]

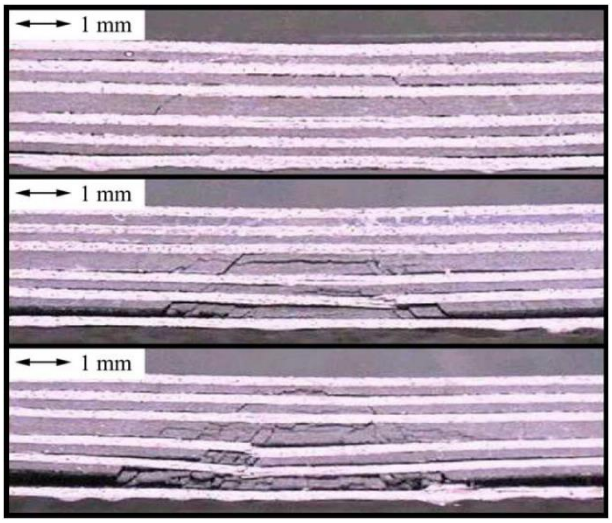

Fig. 6. Optical micrographs of the section at the impact point of a cross-ply CFRP laminate tested at 3 J. Top: RT, middle: -60 °C, bottom: -150 °C. (Reproduced by permission of the copyright holder from [184])

Some authors have reported improved impact behaviour at low and cryogenic temperatures, but these works investigated 3D integrated woven sandwich structures [185–187], tubes [188], 3D multiaxial warp knitted [189,190] or stitched laminates [191]. In these cases, the fibres with increased strength at CT take up the load-bearing role in the out-of-plane direction. Thus, the role of brittle resin with less ductility has less effect on the impact behaviour. Furthermore, thermoplastic resins can also increase the absorbed energy and impact strength compared to thermoset materials [19,192].

At low impact energy, the bending of fibres and the resin are responsible for energy absorption, where the latter results in lower absorbed energy at RT. However, at high impact energy, the fibre breakage becomes the main contributor and the structure can absorb more energy at CT [71,184,193–196]. In the high energy cases the fibre

contribution is further enhanced by the increased fibre-resin interface strength at CT (see Section 2.5), which mitigates the fibre pull-out mechanism during damage propagation and instead forces fibre fracture [197]. Table 9 summarises the effects of low and cryogenic temperatures on the impact behaviour of composites.

Table 9. Summary of the effect of low and cryogenic temperatures on impact behaviour of composites

Resin	Fibre	Structure	T [K]	Property change compared to RT	Ref.
Thermoset resin – Carbon fibre					
Epoxy (R608)	CF (M40)	UD	77	I↑	[28]
Epoxy (3501-6)	CF (AS4)	QI and cross-ply laminates from UD	123	E_{abs}↑	[184]
Epoxy (8552)	CF (AS4)	Woven	123	E_{abs}↓ (low impact energy) ↑ (high impact energy)	[184]
VE	CF	UD	173	E_{abs}↑130%	[56]
VE	CF	Woven	223	E_{abs}↓	[71]
VE (510A)	CF (T700)	Woven	223	E_{abs}↓ (low impact energy) ↑ (high impact energy)	[195]
Thermoset resin – Glass fibre					
Epoxy	GF	Woven	223	E_{abs}↓3% (low impact energy) ↑8% (high impact energy)	[193]
Epoxy	GF (E-glass)	Woven	223	E_{abs}↓ (low impact energy) ↑ (high impact energy)	[194]
Epoxy (CY225)	GF (E-glass)	QI laminate from UD	213	E_{abs}↓ (low impact energy) ↑ (high impact energy)	[196]
Epoxy (GY251)	GF	Woven	100	E_{abs}↓20%	[197]
Epoxy (GY251)	GF	Woven	199	E_{abs}↓12%	[197]
Epoxy (RIM135)	GF (E-glass)	3D MWK (Type C)	77	I↑36% (transverse Charpy test)	[189]
Epoxy (RIM135)	GF (E-glass)	3D MWK (Type A)	77	I↑43% (normal Charpy test)	[190]
Thermoset resin – Other fibre					
Epoxy	AF+GF	Woven	223	E_{abs}↓4% (low impact energy) ↑8% (high impact energy)	[193]
Thermoplastic resin					
PEEK	CF (CF30)	Short fibre	198	E_{abs}↓	[182]

PEEK	GF	Chopped fibre	20	I↑32%	[19]
PEEK	GF	Chopped fibre	77	I↑19%	[19]
PP (HP500 M)+nanoclay	Basalt	Chopped fibre	77	I↓8%	[183]
PUR	GF (E-glass)	Woven	223	E_{abs}↑	[192]

QI: Quasi-isotropic

CAI strength is also reduced at low and cryogenic temperatures [193,195,198,199]. This occurs because the damage is more significant in specimens impacted at cold temperatures and the increased compressive strength measured on pristine specimens (see Section 2.1) cannot overcome this effect.

2.5. Thermal expansion

Thermal expansion is the driving phenomenon affecting the mechanical behaviour of composites at cryogenic and low temperatures. The difference in the CTE of fibres and resins is well known, but its effect is usually addressed at the ply level instead of the constituent level. This approach is generally sufficient to predict the thermal residual stresses and deformation of structures due to cooldown from cure to room temperature. In this case ΔT is typically between 95 °C and 155 °C with common 120 °C and 180 °C cure epoxies. However, ΔT can be 450 °C in the case of a LHe COPV, which can initiate matrix cracking without the application of mechanical loading as a result of excessive thermal strains.

Furthermore, there is a difference between the CTE of the fibres in the longitudinal and transverse directions [200]. In the direction of the fibre axis, aramid fibres and most carbon fibres expand during cooldown, whereas glass and basalt fibres contract.

In the transverse direction, aramid, glass and basalt fibres contract, and carbon fibres expand [1,82]. When combined with the resin, a complex stress state emerges (see Fig. 7). The resin contraction and the carbon fibre transversal expansion generates compressive stresses on the fibre-resin interface, which increases the interface strength. This phenomenon is considered as a primary factor responsible for the improved mechanical properties of composites at CT, described in Section 2.1. As the CTE of the resin is usually one magnitude larger than that of fibres, and therefore it contracts more significantly, the same mechanism exists with transversally contracting aramid and glass fibres. It is also believed that the compressive stresses developed along the axis of longitudinally expanding fibres alleviate the tensile mechanical loading and result in higher ultimate tensile strength [64]. However, the increased tensile strength is not exclusive to fibres with negative longitudinal CTE (see Section 2.1).

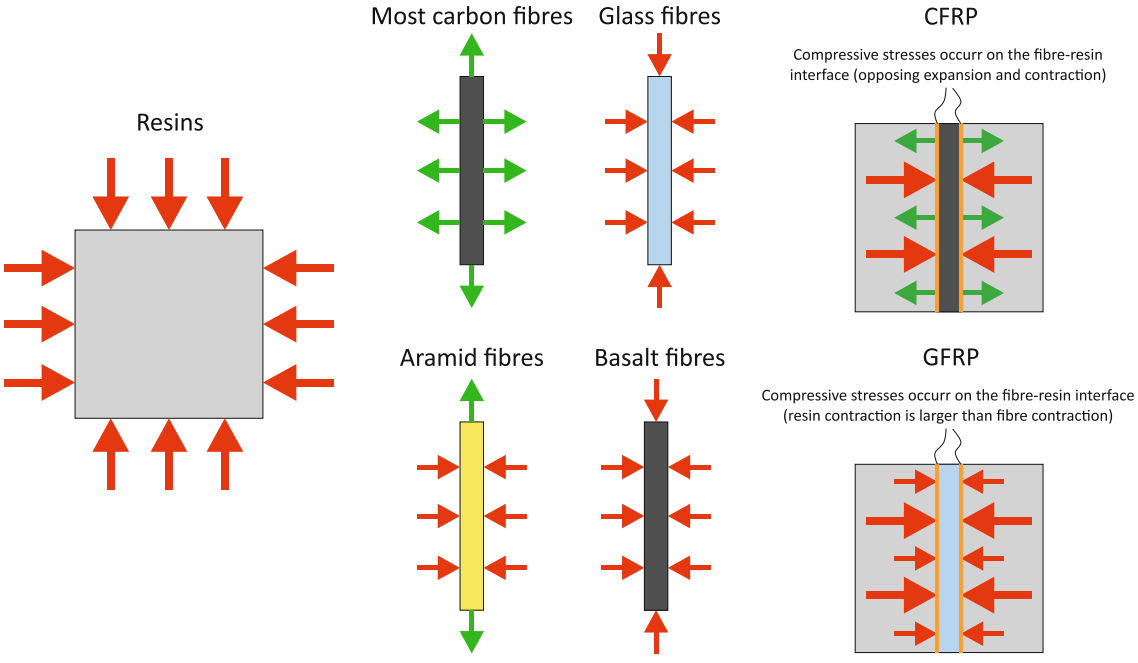

Fig. 7. Deformation during cooldown on resins, fibres and composites.

There is also a CTE difference within the structure of a fibre. A carbon fibre consists of an inside so-called “proper fibre” with negative CTE, which is embodied by an outer shell called “disordered structure” with positive CTE. Due to the contraction of the outer layer and the expansion of the proper fibre at cryogenic temperatures, the outer layer develops cracks, which subsequently increase the surface roughness of the fibre, see Fig. 8 [201–204]. The increased roughness further enhances the interfacial strength between the fibre and the resin due to mechanical interlocking.

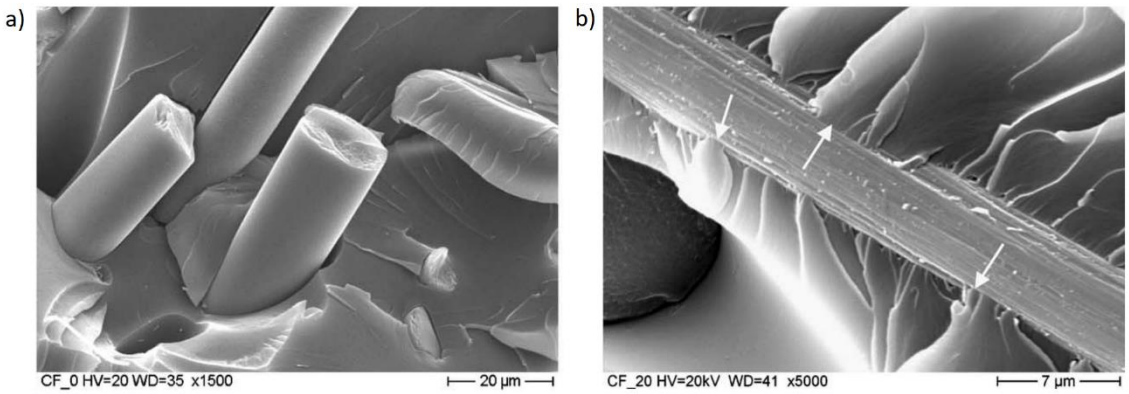

Fig. 8. 7. Fracture surfaces of CF/epoxy composite three-point bending specimens: a) untreated b) cryogenic treated in liquid nitrogen for 10 min. (Reproduced by permission of the copyright holder from [202]. Selected images are cropped from the original figure.)

Finally, the CTE is also temperature-dependent. For resins, it decreases with decreasing temperature [205–207] and it has a higher sensitivity than fibres [208]. The CTE of glass and aramid fibres also decreases with decreasing temperature, but in the case of carbon fibres, it increases with decreasing temperature (Fig. 9) [1,41,208]. For a more detailed, molecular level discussion and review about the temperature dependence of

CTE, the reader is referred to [207]. Thermal cycling also affects CTE at lower temperatures [4,119,209,210].

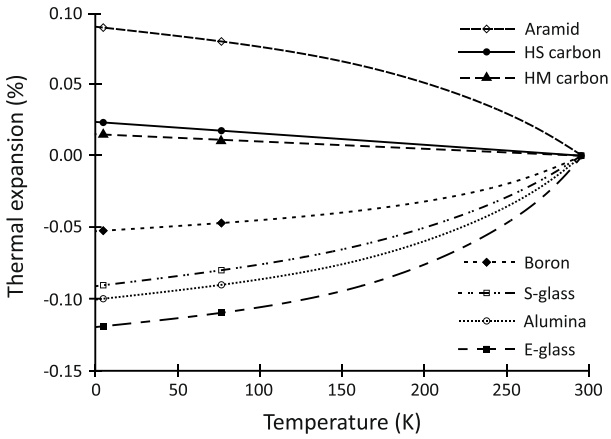

Fig. 9. Thermal expansion of UD fibre-reinforced laminates. (Reproduced by permission of the copyright holder from [1]. Original figure redrawn.)

Using a low cure temperature (120 °C) instead of a high one (180 °C) on the same resin can increase the transverse CTE of the UD lamina by 38% and the CTE of the woven lamina by 91%, respectively. This is due to the lower levels of crosslink density. However, in both cases, the 60 °C lower ΔT outweighed the effect of higher thermal expansion coefficient and resulted in lower crack density when the specimens were cooled down to -100 °C [211].

Woven plies possess a unique property, where the out-of-plane thermal expansion of the lamina is higher than the expansion of the pure resin, which cannot be described by the rule of mixtures. This can occur because the fibres apply in-plane kinematic constraints on the resin, which prevents it from in-plane expansion. However, the volume of the resin is conserved and the expansion can only occur out-of-plane [212,213].

On a structural level, near-zero CTE can be achieved at cryogenic temperatures by hybridising carbon and glass fibre plies [214] or off-angle (30°) plies [133,215] in the laminate. Also, the braid angle can be altered in braided composites to produce a near-zero configuration [72].

Another way to mitigate thermal stress is to use single polymer composites, where the reinforcement and the resin are made of the same thermoplastic material, such as polypropylene (PP) [67].

2.6. Thermal conductivity

Cryogenic structures must be insulated from the environment in order to ensure their operation, reduce freezing cost and in the case of pressure vessels, prevent boiling of the propellant. The lower the thermal conductivity (κ) of the composite structure, the more efficient the insulation becomes. Lower values of κ leads to lower thermal stresses in the support structure away from the cryogenic surface. Hence, an important measure of thermal behaviour of composites are their ratios of strength and stiffness to thermal conductivity, which is several times higher than for metals [5,7].

The thermal conductivity of composites is a temperature-dependent material property, with fibres having higher sensitivity to temperature than resins [216][216]. Between 4.2 K and 77 K, κ remains constant regardless of the fibre content in CFRPs, but at a higher temperature range (77 K – 300 K) the conductivity increases with increasing fibre content [5]. At temperatures above about 30K glass and aramid fibres have the lowest κ, whereas below this temperature the conductivity of carbon fibres becomes lower [1,2], see Fig. 10. Because of this, when accounted for the strength and

stiffness to thermal conductivity ratios, hybrid structures can become the most suitable. An example of this are straps and struts having CT and RT at different ends. At the CT end, carbon fibre composites, and at the RT end, glass or aramid fibre composites have higher strength and stiffness to thermal conductivity ratios [2,14]. At very low temperatures below 4 K, Ventura et al. investigated Zylon and aramid fibres and glass fibre composites [217–221]. They also assembled a data bank for several neat and toughened polymer materials down to 4 K [222], Runyan et al. collected down to 0.3 K [223] and Kramer et al. [224] down to <1 K for different composites.

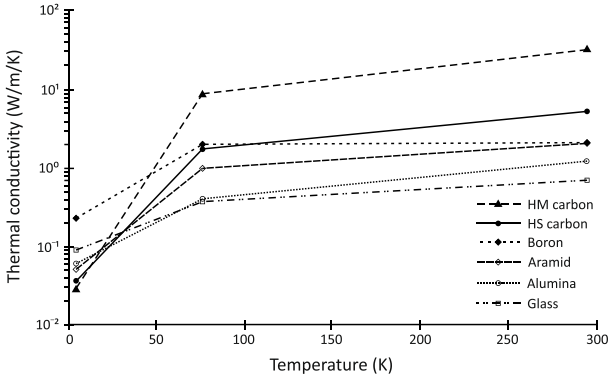

Fig. 10. Thermal conductivity of UD fibre-reinforced laminates. (Reproduced by permission of the copyright holder from [2]. Original figure redrawn.)

Some authors documented glass and carbon fibre epoxy composites to have about 10% higher conductivity in the longitudinal direction, compared with the transverse direction [48,225,226], others reported that this is an order of magnitude for carbon fibre/epoxy [227], and that it can be two orders of magnitude higher for certain material systems, such as BMI resin with various carbon fibres [228].

Evseeva et al. measured the thermal conductivity of carbon fibre/epoxy composites after thermal cycling and found that κ decreases with increasing cycle times due to matrix cracking. The reduction was more significant in the fibre direction [227].

2.7. Tribology and wear

To improve the wear behaviour and reduce the friction of polymers, it is necessary to reduce the adhesion to the counterpart material and enhance the stiffness, hardness and compressive strength of the polymer [229]. As discussed in Section 2.1, with decreasing temperature the modulus and strength of the resin increases, and hardness increase at cold temperatures was reported in [26,230,231]. These effects mean that at CT, the material deforms less and establishes connection with the counter part on a smaller contact area, which leads to reduced friction [229].

Improved wear performance with decreasing temperature, or as a result of cryogenic treatment, was reported in the literature for single Kevlar fibres [40], as well as for various neat polymers [230–232], GF reinforced Polytetrafluoroethylene (PTFE) composites [233], hybrid PTFE/Kevlar fabric reinforced phenolic resin composites [234] and CF reinforced PTFE and PEEK composites [235].

Some authors reported a reduction in friction down to 77 K followed by increase between 77 K and 4.2 K [231,233]. This is believed to be as a results of the cryogen used, as LN_2 has better cooling efficiency than He gas [233].

In some cases, short fibre reinforcement improved the frictional performance at RT, but in turn decreased it at CT compared to the neat resin case [230,236]. According to Indumathi et al. [230], this can be attributed to interfacial debonding between the

resin and fibre reinforcement at CT. This finding emphasises the importance of coupon level testing instead of constituent level testing: whereas the neat resin performs better at CT and the fibre-reinforced resin performs better than the neat one at RT, the combination of the two parameters in fact can reduce the wear performance.

2.8. Permeability

COPVs are one of the main areas of cryogenic composite applications and are extensively investigated in the literature due to their weight saving potential compared to metallic pressure vessels. However, the permeability of composite materials is often a limiting factor in cryotanks [237]. Permeability is both a molecular and microstructural property: diffusion is the phenomenon responsible for propellant atoms passing through the material; whereas leak is caused by the presence of layup-dependent crack paths in the laminate [238] (Fig. 11). Diffusion is usually negligible compared to leakage [239], but it has a time lag tendency and should be measured accordingly [240].

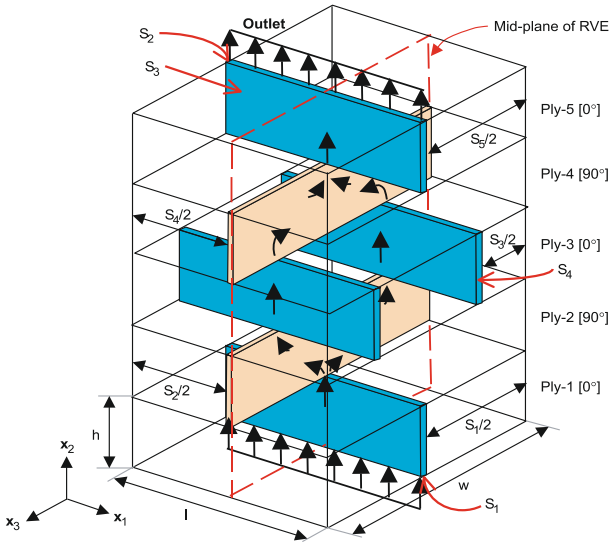

Fig. 11. Crack induced pathway through a laminate (Reproduced by permission of the copyright holder from [241])

Considering purely thermal effects, gases have lower viscosity at cryogenic temperature, which increases flow rate [241]. However, this effect is overthrown by their lower molecular kinetic energy at cold temperatures resulting in lower overall flow rate [242]. However, thermomechanical effects at CT cause thermal stresses and subsequent matrix cracking in the structure. As the cracks develop and interconnect with each other across the laminate, leakage paths emerge. The presence of these cracks, and their increasing density with decreasing temperature and increasing thermal cycles, increase the overall permeability of the material, regardless of the thermodynamically preferable behaviour of gases at CT [124,132,243–246]. However, if the crack density and size of leakage paths plateau at a certain temperature, further decreasing the temperature can decrease permeability due to reduced molecular motion [240].

Yokozeki et al. investigated the permeability of laminates in tension with different ply orientations between 0° and 90° plies. Plies with 30° angle contained longer cracks and developed networks, leading to higher leakage than plies with 45° and 60° orientations, which only developed shorter, unconnected “stitch” cracks [136]. Compared to long cracks and delaminations, unconnected microcracks are preferable in order to prevent the occurrence of leakage paths [247–249]. For laminates having only 0° and angle plies, the aforementioned tendency switched, and smaller angles led to higher a leak conductance [250,251]. The use of a quasi-isotropic stacking sequence showed higher crack density than cross-ply laminates in Grogan et al.’s work [123]. Bechel and Kim also highlighted the importance of 90° difference between adjacent plies in order to reduce crack propagation [53]. Similar laminates with small changes in orientation between plies have a lower tendency for micro-crack initiation [53,252]. Choi and Sankar reported reduced permeability using woven plies compared to UD plies [253], but these results are not fully comparable due to the thickness and strength difference between the two materials.

Permeability of composite laminates exposed to cryogenic temperatures can be reduced by using toughened epoxy [53] or BMI resins [254], or thermoplastic resins [255,256], which have increased fracture toughness and can reduce matrix cracking.

Metal liners can be used (type III COPV) instead of all-composite structures (type IV COPV), but the metal-composite interface generates further difficulties in manufacturing and increases weight [257]. Therefore, research was carried out on

replacing the solid metal liners with lighter, composite-compatible and non-permeable films [258–264].

2.9. Resin fillers

It has been demonstrated above that cryogenic temperatures have a positive effect on the properties of resins in most cases. However, their failure strain and ductility reduces and composites have poor impact resistance at cold temperatures. Mainly driven by the mitigation of these effects, there is a growing interest in toughening the matrix with fillers. Nevertheless, the reinforcements can also affect other properties: improved strength and modulus, fatigue performance, fracture toughness, wear properties; and decrease thermal conductivity and CTE. The summary of the effect of resin fillers on the material properties of resins at low and cryogenic temperatures can be seen in Table 10, and only the main characteristics related to the properties at lower temperatures are highlighted below.

Table 10. Summary of the effect of resin fillers on material properties at low and cryogenic temperatures. In those cases, where several amounts of fillers were investigated, only the most beneficial case is cited

Resin	Filler	Content	T [K]	Property change compared to RT	Ref.
Thermoset resin					
Epoxy (CYD-128)	PEG	Various wt%	77	E↑50% (5 wt%), I↑9% (10 wt%), S_T↑68% (15 wt%), ε↓30% (10 wt%)	[18]
Epoxy (YD-128)	R-MWCNT	0.5 wt%	77	E↑68%, I↓34%, S_T↑24%, ε↓	[30]
Epoxy (YD-128)	O-MWCNT	0.5 wt%	77	E↑55%, I↓40%, S_T↑25%, ε↓	[30]
Epoxy (YD-128)	Fe_3O_4/O-MWCNT	0.5 wt%	77	E↑54%, I↓42%, S_T↑26%, ε↓	[16]

Epoxy (YD-128)	GO	0.5 wt%	77	E↑43%, I↓38%, S_T↑24%, ε↓15%	[147]
Epoxy (YD-128)	GO/Fe_3O_4	0.5 wt%	77	E↑44%, I↓40%, S_T↑23, ε↓20%	[147]
Epoxy (YD-128)	Core–shell rubber	Various wt%	77	E↑74% (1.0 wt%), I↓31% (0.5 wt%), S_T↑41% (0.5 wt%), ε↓	[31]
Epoxy (YD-128)	PBT	1.0 wt%	77	I↓44%	[181]
Epoxy (YD-128)	PC	1.0 wt%	77	I↓46%	[181]
Epoxy (YD-128)	PEI	0.5 wt%	77	I↓45%	[181]
Epoxy (DGEBA)	AlOOH	2.5 wt%	77	G_{IIC}↑	[156]
Epoxy (DGEBF)	Nano-ZrO_2	Various g / 100 g epoxy	90	E↑201% (5 g), K_{IC}↑19% (5 g), S_T↑62% (1 g), ε↓63% (1 g)	[24]
Epoxy (DGEBF)	HTDE-2	10 wt%	77	I↑, S_T↑, ε↑	[25]
Epoxy (DGEBF)	Nano-rubber	15 phr	77	E↑100%, S_T↑83%, ε↓57%	[27]
Epoxy (DGEBF)	MWCNT	Various wt%	77	E↑70% (0.02 wt%), I↓20% (0.02 wt%), S_T↑60% (0.5 wt%), ε↓47% (2 wt%)	[20]
Epoxy (DGEBF)	CCNT	1 wt%	77	E↑41%	[26]
Epoxy (WSR615)	Graphene nanosheets	Various wt%	77	E↑, I↓4%, S_T↑	[29]
Epoxy (828)	GO-PDA	Various wt%	153	E↑155% (0.5 wt%), K_{IC}↑17% (2.0 wt%), S_T↑ (0.05 wt%), ε↓ (0.5 wt%)	[32]
DCPD	Carbon nanocoil	1 wt%	77	E↑, S_T↑, ε↓	[265]
DCPD	Carbon nanofibre	0.5 wt%	77	E↑, S_T↑, ε↓	[33]
Thermoplastic resin					
PC	MWNT	Various vol%	77	E↑87% (1.0 vol%), S_T↑135% (1.7 vol%), ε↓ (1.0 vol%)	[36]
PES	GO	0.5 wt%	77	E↑, E_F↑, S_F↑, S_T↑, ε↓, ε_F↓	[17]
PP (HP500 M)	Nanoclay	5 wt%	77	I↓12%	[183]

AlOOH: Nanosheet boehmite, CCNT: Coiled carbon nanotube, FGS: Functionalized graphene sheet, GO: Graphene oxide, GO-PDA: Graphene oxide/poly p-phenylenediamine, HTDE-2: Polyester hyperbranched epoxy resin, O-MWCNT: Oxidised multi-walled carbon nanotube, PEG: Polyethylene glycol, R-MWCNT: Raw multi-walled carbon nanotube

The increase of the binding forces at CT increases strength. This does not only occur between the molecules of the epoxy, but also between the molecules of the filler and

resin [16]. Moreover, additives increase the crosslink density of the polymer, which further increases strength [27], and the subsequently reduced chain mobility provides increased modulus. The mechanical locking of the polymer chains with the addition of fillers can enhance the available free space and free volume (see Section 2.3) in the matrix and improve fracture toughness at CT [148]. The same locking mechanism causes CTE reduction, which prevents the shrinkage of the resin molecules; combined with the negative CTE of the additives, which contributes to lower overall CTE based on the rule of mixtures. However, excessive content of fillers can increase the CTE of the resin [31].

A side effect of using additives with the resin is the change of glass transition temperature (T_g). Usually the cure temperature is used as the stress free temperature for thermal residual stress calculations, however, the glass transition temperature is considered more accurate as the solidification occurs at this temperature [266]. Resin fillers usually increase T_g, which in turn increases ΔT and contributes to higher thermal residual stresses [181,267,268]. Thermal cycling can also increase the glass transition temperature [119,140].

The chosen wt% of the fillers and operating temperatures of the structure is critical. In some cases, the additive at a certain wt% can provide maximised property improvement at RT, but have a different optimal wt% at LT or CT [27]. Thus, it might be necessary to “give up” additional improvement at RT in order to achieve the best improvement at cold temperatures.

3. Experimental testing

When using composites at cryogenic temperatures, the engineer must not only account for the differences in material properties compared to room temperature conditions, but also for the challenges related to the experimental testing at cold temperatures. This section highlights features and practices unique to cryogenic experimental procedures.

3.1. Manufacturing method and specimen configuration

Filament winding is the primary manufacturing method for COPVs. However, the manufacturing quality and therefore the performance can differ from laminated components. Therefore, filament wound flat specimens were used by Noorda et al. [269].

The volume restriction of cryogenic dewars fitted to testing machines requires the use of coupons with reduced size. This can lead to specimens with out of range dimensions and different shape (e.g. dog bone instead of rectangular [270]) to those specified by standards, therefore increasing the sensitivity of specimens to boundary conditions such as free-edge effects and clamping [78]. Several authors reported inconsistency in material properties measured at CT in the literature [22,55,124,271], and the deviation from standards is believed to be one reason for this.

Charalambous et al. used asymmetric cut-ply coupons for fatigue delamination growth measurement, as this configuration does not need monitoring of the delamination length during fatigue testing [108]. Shindo and his co-workers proposed using open hole testing for indirect measurement of tensile strength, as these specimens fail at

lower load and are not affected by the stress concentration near clamping [55,272]. Shindo et al. noted that compact tension coupons are preferred because they require the least amount of test material to evaluate crack growth behaviour [22]. Pan et al. achieved reduced fixture size by a self-designed jig [273]. Four-point end-notched flexure specimens can stabilise crack-growth at CT compared to three-point end-notched flexure testing [157]. In order to eliminate poor adhesive performance, Oliver and Johnson used bolted DCB specimens [170] and Coronado el al. used notched DCB specimens [114]. Kim et al. used emery cloth instead of woven glass fibre for tab material on tensile test coupons, as the latter can separate due to the CTE difference between GFRP and CFRP [41,47]. Furthermore, to prevent the slippage, wedge tabs can be used [43].

3.2. Testing medium

The desired temperature can be achieved by submerging the specimen in cryogenic liquid, evaporating cryogenic liquid in an environment chamber or using heat exchangers while the specimen is subjected to air or vacuum (in-situ conditioning). Whereas these methods represent achievable temperature ranges, in some cases there is an overlap and the same experiment can be performed using different techniques (such as LN_2 and He gas for 77 K [233]). It is crucial to use the medium representative of the operational condition of the component, as different approaches can lead to differences in measured material properties. This is due to the different cooling efficiency of the medium, which must counteract the heat dissipated at material failure and during abrasion. The type of medium also affects the permeability

measurement [274]. The presence of an oxidative medium (testing in air instead of nitrogen or vacuum) can degrade material properties and cause matrix shrinkage [121]. Yu et al. carried out impact testing on a specimen submerged in cryogen, but its effect was not discussed [275].

The cooled down specimen can also be removed from the medium and tested in room temperature (ex-situ conditioning), assuming that the temperature of the component does not change significantly in the meantime. However, this method is not recommended, especially if the specimen gets into contact with the RT testing rig, causing an elevated rate of temperature change and thermal residual stresses in the coupon.

The submerging method must also be taken into account. A typical application of cryogenic composites is COPVs containing cryogenic fuel. A temperature difference can be present between the inside and outside surface of the tank, e.g. fuelling of a launch vehicle in the launch pad. This leads to a temperature gradient and therefore strain and stress gradients across the thickness of the specimen, which can induce material failure [53,54]. However, this effect is disregarded in many cases as experiments are usually carried out by submerging the coupon in the cryogenic medium and testing it when the desired temperature is achieved across the whole specimen. Furthermore, the free-edge effect can disappear because of a lack of thermal gradient at the coupon edge but an existing thermal gradient away from the edge. Similar stress gradients can be achieved with resin edge treatment [238]. The free-edge effect is also related to

laminate thickness, as 16 ply laminates crack more than 8 plies due to a larger stress gradient [123].

3.3. Inspection

The liquid cryogenic medium eliminates the possibility of visual observation and even if an environmental chamber is used, the presence of gas can interfere with digital image correlation results [276]. Therefore, acoustic emission is a preferred method for observation of failure at cryogenic temperatures. However, the background noise can be too high due to the boiling of the liquid cryogen [266,277].

Thermal expansion of strain gauges and the adhesive used to bond them on the specimen can lead to disengagement of the gauges. Therefore, cryogenic adhesives [167,278] and appropriate calibration is recommended. Aoki et al. also reported better accuracy with clip-on extensometers [3]. Crack gauges can be used for delamination length measurement, as the data is acquired based on resistance change in the gauge and visual access is not required [100].

4. Conclusions

The properties of composite materials subjected to low and cryogenic temperatures have been reviewed. Generally, cold temperature has a positive effect on composites resulting in improved strength, modulus, fatigue and thermal properties. Contrarily, it causes a reduction in ductility, leading to lowered failure strain, fracture toughness and impact resistance. Some of these trends were identified by the review articles assembled almost three decades ago. However, the literature published since then has not only extended coverage to a wider range of materials, manufacturing methods and

experimental conditions, but also provided understanding of the underlying failure mechanisms occurring in the material, down to the molecular level.

The authors outline the following areas of interest for future research of low temperature and cryogenic composites:

- To address the decreased resin ductility, fillers have been shown as a promising approach. Most of the related literature only focused on the behaviour of resins, but implementing these additives into fibre reinforced composite material systems should be undertaken.
- Microcracking of the laminate due to thermal shock and cycling is a limiting factor in permeability. Moreover, it can also cause a reduction in mechanical properties, which is a less understood phenomenon. Further studies are needed to understand this connection and provide predictive capabilities for the design of cryogenic structures.
- New manufacturing procedures are emerging, and the characterisation of the resultant products at cryogenic temperatures is an untapped field. These include braided and 3D woven composites, which are addressed in this review. However, to the authors' best knowledge, there is no published literature on the cryogenic behaviour of 3D printed composite materials.
- There is a great debate over the appropriate methods of testing at cryogenic temperatures as standards usually do not address these conditions. Therefore, results from different test campaigns generate scatter across the literature. Not only do the methods need standardising, but improvement is also required with the

harmonisation of testing and inspection apparatus to eliminate the need for in-house built equipment.

Acknowledgement

This research did not receive any specific grant from funding agencies in the public, commercial, or not-for-profit sectors. Richard Butler holds the Royal Academy of Engineering – GKN Aerospace Composites Research Chair.

References

[1] Reed RP, Golda M. Cryogenic properties of unidirectional composites. Cryogenics 1994;34:909–28. doi:10.1016/0011-2275(94)90077-9.

[2] Schutz J B. Properties of composite materials for cryogenic applications. Cryogenics 1998;38:3–12. doi:10.1016/S0011-2275(97)00102-1.

[3] Aoki T, Kumazawa H, Ishikawa T, Morino Y. Mechanical performance of CF/polymer composite laminates under cryogenic conditions. 41th AIAA/ASME/ASCE/AHS/ASC Struct. Struct. Dyn. Mater. Conf. Exhib., 2000. doi:10.2514/6.2000-1605.

[4] Fu SY, Li Y, Zhang YH, Pan QY, Huang CJ. Cryogenic properties of polymer composite materials - a review. Proc. Twent. Int. Cryog. Eng. Conf., 2005. doi:10.1016/B978-008044559-5/50215-5.

[5] Horiuchi T, Ooi T. Cryogenic properties of composite materials. Cryogenics 1995;35:677–9. doi:10.1016/0011-2275(95)90887-L.

[6] Sethi S, Ray BC. Mechanical behavior of polymer composites at cryogenic temperatures. Polym. Cryog. Temp., Berlin: Springer; 2013, p. 59–113. doi:10.1007/978-3-642-35335-2_4.

[7] Li LF, Zhang YT, Li YY. Development of cryogenic structural materials. Twent. Int. Cryog. Eng. Conf., 2005.

[8] Yano O, Yamaoka H. Cryogenic properties of polymers. Prog Polym Sci 1995;20:585–613. doi:10.1016/0079-6700(95)00003-X.

[9] Ray BC, Rathore D. Durability and integrity studies of environmentally conditioned interfaces in fibrous polymeric composites: Critical concepts and comments. Adv Colloid Interface Sci 2014;209:68–83. doi:10.1016/j.cis.2013.12.014.

[10] Kasen MB. Cryogenic properties of filamentary-reinforced composites: an update. Cryogenics 1981;21:323–40. doi:10.1016/0011-2275(81)90015-1.

[11] Kasen MB. Mechanical and thermal properties of filamentary-reinforced structural composites at cryogenic temperatures 1: Glass-reinforced composites. Cryogenics 1975;15:327–49. doi:10.1016/0011-2275(75)90079-X.

[12] Kasen MB. Mechanical and thermal properties of filamentary-reinforced structural composites at cryogenic temperatures 2: Advanced composites. Cryogenics 1975;15:701–22. doi:10.1016/0011-2275(75)90085-5.

[13] Kasen M. Properties of Filamentary-Reinforced Composites at Cryogenic Temperatures. In: Wu E, editor. Compos. Reliab., West Conshohocken: ASTM International; 1975, p. 586–611. doi:10.1520/STP32335S.

[14] Haider G, Khan ZA. Cryogenic composite supports: a review of strap and strut properties. Cryogenics 1997;37:233–50. doi:10.1016/S0011-2275(97)00004-0.

[15] Reed RP, Golda M. Properties of cold-to-warm support straps. Cryogenics 1998;38:39–42. doi:10.1016/S0011-2275(97)00107-0.

[16] He Y, Yang S, Liu H, Shao Q, Chen Q, Lu C, et al. Reinforced carbon fiber laminates with oriented carbon nanotube epoxy nanocomposites: Magnetic field assisted alignment and cryogenic temperature mechanical properties. J Colloid Interface Sci 2018;517:40–51. doi:10.1016/j.jcis.2018.01.087.

[17] Li F, Hua Y, Qu CB, Xiao HM, Fu SY. Greatly enhanced cryogenic mechanical properties of short carbon fiber/polyethersulfone composites by graphene oxide coating. Compos Part A Appl Sci Manuf 2016;89:47–55. doi:10.1016/j.compositesa.2016.02.016.

[18] Feng Q, Yang J, Liu Y, Xiao H, Fu S. Simultaneously enhanced cryogenic tensile strength, ductility and impact resistance of epoxy resins by polyethylene glycol. J Mater Sci Technol 2014;30:90–6. doi:10.1016/j.jmst.2013.08.016.

[19] Chu XX, Wu ZX, Huang RJ, Zhou Y, Li LF. Mechanical and thermal expansion properties of glass fibers reinforced PEEK composites at cryogenic temperatures. Cryogenics 2010;50:84–8. doi:10.1016/j.cryogenics.2009.12.003.

[20] Chen ZK, Yang JP, Ni QQ, Fu SY, Huang YG. Reinforcement of epoxy resins with multi-walled carbon nanotubes for enhancing cryogenic mechanical properties. Polymer 2009;50:4753–9. doi:10.1016/j.polymer.2009.08.001.

[21] Ward IM, Sweeney J. Mechanical properties of solid polymers. 3rd ed. John Wiley & Sons, Ltd.; 2013. doi:10.1002/9781119967125.

[22] Shindo Y, Inamoto A, Narita F. Characterization of mode I fatigue crack growth in GFRP woven laminates at low temperatures. Acta Mater 2005;53:1389–96. doi:10.1016/j.actamat.2004.11.032.

[23] Yang L, Li Z, Xu H, Wu Z. Prediction on residual stresses of carbon/epoxy composite at cryogenic temperature. Polym Compos 2019. doi:10.1002/pc.25202.

[24] Li J, Peng C, Li Z, Wu Z, Li S. The improvement in cryogenic mechanical properties of nano-ZrO2/epoxy composites via surface modification of nano-ZrO2. RSC Adv 2016;6:61393–401. doi:10.1039/c6ra08047b.

[25] Li J, Wu Z, Huang C, Huang R, Li L. Mechanical behaviors of hyberbranched epoxy toughened bisphenol F epoxy resin for cryogenic applications. 2013 Jt. Cryog. Eng. Int. Cryog. Mater. Conf., 2013. doi:10.1063/1.4860614.

[26] Lau KT, Wong TT, Leng J, Hui D, Rhee KY. Property enhancement of polymer-based composites at cryogenic environment by using tailored carbon nanotubes. Compos Part B Eng 2013;54:41–3. doi:10.1016/j.compositesb.2013.03.044.

[27] Zhao Y, Chen ZK, Liu Y, Xiao HM, Feng QP, Fu SY. Simultaneously enhanced cryogenic tensile strength and fracture toughness of epoxy resins by carboxylic nitrile-butadiene nano-rubber. Compos Part A Appl Sci Manuf 2013;55:178–87. doi:10.1016/j.compositesa.2013.09.005.

[28] Shi H, Sun B, Liu Q, Yang Z, Zhang Y. Properties of cryogenic epoxy resin matrix composites prepared by RTM process. 17th Eur. Conf. Compos. Mater., 2015.

[29] Shen XJ, Liu Y, Xiao HM, Feng QP, Yu ZZ, Fu SY. The reinforcing effect of graphene nanosheets on the cryogenic mechanical properties of epoxy resins. Compos Sci Technol 2012;72:1581–7. doi:10.1016/j.compscitech.2012.06.021.

[30] He Y, Zhang L, Chen G, Li X, Yao D, Lee JH, et al. Surface functionalized carbon nanotubes and its effects on the mechanical properties of epoxy based composites at cryogenic temperature. Polym Bull 2014;71:2465–85. doi:10.1007/s00289-014-1202-6.

[31] He YX, Sang YF, Zhang L, Yao DH, Sun KB, Zhang YQ. Coefficient of thermal expansion and mechanical properties at cryogenic temperature of core–shell rubber particle

modified epoxy. Plast Rubber Compos 2014;43:89–97. doi:10.1179/1743289814y.0000000074.

[32] Hussein A, Sarkar S, Lee K, Kim B. Cryogenic fracture behavior of epoxy reinforced by a novel graphene oxide/poly(p-phenylenediamine) hybrid. Compos Part B Eng 2017;129:133–42. doi:10.1016/j.compositesb.2017.07.085.

[33] Sanada K, Sanga H, Shindo Y. Cryogenic tensile and fracture properties of carbon nanofiber/poly- dicyclopentadiene composites fabricated by ultrasonic method. J Compos Mater 2012;46:1431–8. doi:10.1177/0021998311418851.

[34] Zhang Z, Hartwig G. Low-temperature viscoelastic behavior of unidirectional carbon composites. Cryogenics 1998;38:401–5. doi:10.1016/S0011-2275(98)00022-8.

[35] Baschek G, Hartwig G, Zahradnik F. Effect of water absorption in polymers at low and high temperatures. Polymer 1999;40:3433–41. doi:10.1016/S0032-3861(98)00560-6.

[36] Takeda T, Shindo Y, Narita F, Mito Y. Tensile characterization of carbon nanotube-reinforced polymer composites at cryogenic temperatures: experimens and multiscale simulations. Mater Trans 2009;50:436–45. doi:10.2320/matertrans.mbw200817.

[37] Pavlick MM, Johnson WS, Jensen B, Weiser E. Evaluation of mechanical properties of advanced polymers for composite cryotank applications. Compos Part A Appl Sci Manuf 2009;40:359–67. doi:10.1016/j.compositesa.2008.12.009.

[38] Zhang Y, Xu F, Zhang C, Wang J, Jia Z, Hui D, et al. Tensile and interfacial properties of polyacrylonitrile-based carbon fiber after different cryogenic treated condition. Compos Part B Eng 2016;99:358–65. doi:10.1016/j.compositesb.2016.05.056.

[39] Kwon DJ, Wang ZJ, Choi JY, Shin PS, Devries KL, Park JM. Interfacial evaluation of carbon fiber/epoxy composites using electrical resistance measurements at room and a

cryogenic temperature. Compos Part A Appl Sci Manuf 2015;72:160–6. doi:10.1016/j.compositesa.2015.02.007.

[40] Xu F, Fan W, Zhang Y, Gao Y, Jia Z, Qiu Y, et al. Modification of tensile, wear and interfacial properties of Kevlar fibers under cryogenic treatment. Compos Part B Eng 2017;116:398–405. doi:10.1016/j.compositesb.2016.10.082.

[41] Kim MG, Kang SG, Kim CG, Kong CW. Tensile response of graphite/epoxy composites at low temperatures. Compos Struct 2007;79:84–9. doi:10.1016/j.compstruct.2005.11.031.

[42] Shiroshita S, Okamoto K, Komai K. The effect of water-absorption and cryogenic temperature on the strength of ArFRP. Mater Sci Res Int 1998;4:287–93. doi:10.2472/jsms.46.157.

[43] Kumagai S, Shindo Y, Horiguchi K, Takeda T. Mechanical characterization of CFRP woven laminates between room temperature and 4 K. JSME Int Journal, Ser A Solid Mech Mater Eng 2003;46:359–64. doi:10.1299/jsmea.46.359.

[44] Yang B, Yue Z, Geng X, Wang P, Gan J, Liao B. Effects of space environment temperature on the mechanical properties of carbon fiber/bismaleimide composites laminates. Proc Inst Mech Eng Part G J Aerosp Eng 2018;232:3–16. doi:10.1177/0954410017740382.

[45] Yang B, Yue Z, Geng X, Wang P. Temperature effects on transverse failure modes of carbon fiber/bismaleimides composites. J Compos Mater 2017;51:261–72. doi:10.1177/0021998316639122.

[46] Gates TS, Whitley KS, Grenoble RW, Bandorawalla T. Thermal/mechanical durability of polymer-matrix composites in cryogenic environments. 44th AIAA/ASME/ASCE/AHS Struct. Struct. Dyn. Mater. Conf., 2003. doi:10.2514/6.2003-1600.

[47] Kim MG, Kang SG, Kim CG, Kong CW. Tensile properties of carbon fiber composites with different resin compositions at cryogenic temperatures. Adv Compos Mater 2010;19:63–77. doi:10.1163/156855109X434838.

[48] Wei W, Rongjin H, Chuanjun H, Zhao Y, Li S, Laifeng L. Cryogenic performances of T700 and T800 carbon fibre-epoxy laminates. 2015 Jt. Cryog. Eng. Int. Cryog. Mater. Conf., 2015. doi:10.1088/1757-899X/102/1/012016.

[49] Gong M, Wang XF, Zhao JH. Experimental study on mechanical behavior of laminates at low temperature. Cryogenics 2007;47:1–7. doi:10.1016/j.cryogenics.2006.01.018.

[50] Li D sen, Duan H wei, Jiang N, Jiang L. Mechanical response and failure of 3D MWK carbon/epoxy composites at cryogenic temperature. Fibers Polym 2015;16:1349–61. doi:10.1007/s12221-015-1349-2.

[51] Hung P yan, Lau K tak, Qiao K, Fox B, Hameed N. Property enhancement of CFRP composites with different graphene oxide employment methods at a cryogenic temperature. Compos Part A Appl Sci Manuf 2019;120:56–63. doi:10.1016/j.compositesa.2019.02.012.

[52] Islam MS, Melendez-Soto E, Castellanos AG, Prabhakar P. Investigation of woven composites as potential cryogenic tank materials. Cryogenics 2015;72:82–9. doi:10.1016/j.cryogenics.2015.09.005.

[53] Bechel VT, Kim RY. Damage trends in cryogenically cycled carbon/polymer composites. Compos Sci Technol 2004;64:1773–84. doi:10.1016/j.compscitech.2003.12.007.

[54] Bechel VT, Camping JD, Kim RY. Cryogenic/elevated temperature cycling induced leakage paths in PMCs. Compos Part B Eng 2005;36:171–82. doi:10.1016/j.compositesb.2004.03.001.

[55] Mitchell MR, Link RE, Watanabe S, Shindo Y, Takeda T, Narita F, et al. Evaluation of tensile strength of woven carbon/epoxy composite laminates at cryogenic temperatures using the open hole specimens. J Test Eval 2011;39:103132. doi:10.1520/jte103132.

[56] Jia Z, Li T, Chiang F pen, Wang L. An experimental investigation of the temperature effect on the mechanics of carbon fiber reinforced polymer composites. Compos Sci Technol 2018;154:53–63. doi:10.1016/j.compscitech.2017.11.015.

[57] Li D Sen, Zhao CQ, Jiang L, Lu N, Chen L-M, Jiang N. A comparative study on the tensile properties and failure mechanism of 3D MWK composites at room and liquid nitrogen temperature. Polym Compos 2014;35:1294–305. doi:10.1002/pc.22780.

[58] Takeda T, Narita F, Shindo Y, Sanada K. Cryogenic through-thickness tensile characterization of plain woven glass/epoxy composite laminates using cross specimens: Experimental test and finite element analysis. Compos Part B Eng 2015;78:42–9. doi:10.1016/j.compositesb.2015.03.076.

[59] Kumagai S, Shindo Y, Horiguchi K, Narita F. Experimental and finite-element analysis of woven glass-cloth/epoxy laminate tensile specimen at room and low temperatures. Mech Adv Mater Struct 2004;11:51–66. doi:10.1080/15376490490257666.

[60] Shindo Y, Takano S, Narita F, Horiguchi K. Tensile and damage behavior of plain weave glass/epoxy composites at cryogenic temperatures. Fusion Eng Des 2006;81:2479–83. doi:10.1016/j.fusengdes.2006.07.059.

[61] Torabizadeh MA. Tensile, compressive and shear properties of unidirectional glass/epoxy composites subjected to mechanical loading and low temperature services. Indian J Eng Mater Sci 2013;20:299–309.

[62] Li D Sen, Jiang N, Jiang L, Lu N. Experimental study on the bending properties and failure mechanism of 3D multi-axial warp knitted composites at room and liquid nitrogen temperatures. J Compos Mater 2016;50:557–71. doi:10.1177/0021998315579299.

[63] Shindo Y, Takeda T, Narita F. Mechanical response of nonwoven polyester fabric/epoxy composites at cryogenic temperatures. Cryogenics 2012;52:564–8. doi:10.1016/j.cryogenics.2012.07.008.

[64] Huang YK, Frings PH, Hennes E. Mechanical properties of Zylon/epoxy composite. Compos Part B Eng 2002;33:109–15. doi:10.1016/S1359-8368(01)00064-6.

[65] Dalgarno RW, Garnich MR, Andrews EW. Thermal fatigue cracking of an IM7/5250-4 cross ply laminate: Experimental and analytical observations. J Compos Mater 2009;43:2699–715. doi:10.1177/0021998309345315.

[66] Bechel V. Comparison of matrix cracking in high temperature and lower temperature PMCs from cryogenic exposure. 48th AIAA/ASME/ASCE/AHS/ASC Struct. Struct. Dyn. Mater. Conf., 2007. doi:10.2514/6.2007-2080.

[67] Atli-Veltin B. Cryogenic performance of single polymer polypropylene composites. Cryogenics 2018;90:86–95. doi:10.1016/j.cryogenics.2018.01.009.

[68] Wang Q, Jian C, Lida L, Wei N. Effect of cryogenic temperatures on the failure strain and surface morphology of glass fiber. 7th Int. Conf. Key Eng. Mater., 2017. doi:10.1088/1757-899X/201/1/012044.

[69] Bersani A, Canonica L, Cariello M, Cereseto R, Di Domizio S, Pallavicini M. Long term elongation of Kevlar-49 single fiber at low temperature. Cryogenics 2013;54:50–3. doi:10.1016/j.cryogenics.2012.10.005.

[70] Barbero EJ, Cabrera Barbero J. Damage initiation and evolution during monotonic cooling of laminated composites. J Compos Mater 2018;52:4151–70. doi:10.1177/0021998318776721.

[71] Castellanos AG, Cinar K, Guven I, Prabhakar P. Low-velocity impact response of woven carbon composites in arctic conditions. J Dyn Behav Mater 2018;4:308–16. doi:10.1007/s40870-018-0160-8.

[72] Wang H, Cao M, Siddique A, Sun B, Gu B. Numerical analysis of thermal expansion behaviors and interfacial thermal stress of 3D braided composite materials. Comput Mater Sci 2017;138:77–91. doi:10.1016/j.commatsci.2017.06.023.

[73] Liu J, Qiao W, Liu J, Xie D, Zhou Z, Ma L, et al. The compressive responses of glass fiber composite pyramidal truss cores sandwich panel at different temperatures. Compos Part A Appl Sci Manuf 2015;73:93–100. doi:10.1016/j.compositesa.2015.03.004.

[74] Liu J, Zhou Z, Ma L, Xiong J, Wu L. Temperature effects on the strength and crushing behavior of carbon fiber composite truss sandwich cores. Compos Part B Eng 2011;42:1860–6. doi:10.1016/j.compositesb.2011.06.019.

[75] Hufenbach W, Gude M, Böhm R, Zscheyge M. The effect of temperature on mechanical properties and failure behaviour of hybrid yarn textile-reinforced thermoplastics. Mater Des 2011;32:4278–88. doi:10.1016/j.matdes.2011.04.017.

[76] Wang H, Sun B, Gu B. Coupling effect of temperature and braided angle on compressive behaviors of 3D braided carbon–epoxy composite at low temperature. J Compos Mater 2017;51:2531–47. doi:10.1177/0021998316674065.

[77] Li D, Duan H, Jiang L. Cryogenic compression properties and failure mechanism of lightweight 3D MWK carbon fabric reinforced epoxy composites. Fibers Polym

2019;20:642–50. doi:10.1007/s12221-019-8639-z.

[78] Li D Sen, Zhao CQ, Ge TQ, Jiang L, Huang CJ, Jiang N. Experimental investigation on the compression properties and failure mechanism of 3D braided composites at room and liquid nitrogen temperature. Compos Part B Eng 2014;56:647–59. doi:10.1016/j.compositesb.2013.08.068.

[79] Shindo Y, Tokairin H, Sanada K, Horiguchi K, Kudo H. Compression behavior of glass-cloth/epoxy laminates at cryogenic temperatures. Cryogenics 1999;39:821–7. doi:10.1016/S0011-2275(99)00086-7.

[80] Li D sen, Zhao C qi, Jiang L, Jiang N. Experimental study on the bending properties and failure mechanism of 3D integrated woven spacer composites at room and cryogenic temperature. Compos Struct 2014;111:56–65. doi:10.1016/j.compstruct.2013.12.026.

[81] Wu X, Zhang Q, Gu B, Sun B. Influence of temperature and strain rate on the longitudinal compressive crashworthiness of 3D braided composite tubes and finite element analysis. Int J Damage Mech 2017;26:1003–27. doi:10.1177/1056789516648369.

[82] Pan Z, Sun B, Gu B. Thermo-mechanical numerical modeling on impact compressive damage of 3-D braided composite materials under room and low temperatures. Aerosp Sci Technol 2016;54:23–40. doi:10.1016/j.ast.2016.03.027.

[83] Pan Z, Gu B, Sun B. Experimental investigation of high-strain rate properties of 3-D braided composite material in cryogenic field. Compos Part B Eng 2015;77:379–90. doi:10.1016/j.compositesb.2015.03.002.

[84] Wang H, Sun B, Gu B. Finite element analyses on longitudinal compressive behaviors of 3D braided carbon /epoxy composite with different braided angles at low

temperatures. J Text Inst 2019;110:37–49. doi:10.1080/00405000.2018.1460038.

[85] Hirano NY, Takao Y, Wang WX. Effects of temperature on the bearing strength of CF/epoxy pinned joints. J Compos Mater 2007;41:335–51. doi:10.1177/0021998306063374.

[86] Walker SP. Thermal effects on the pin-bearing behavior of IM7/PETI5 composite joints. J Compos Mater 2002;36:2623–51. doi:10.1177/002199802761675557.

[87] Sethi S, Rathore DK, Ray BC. Effects of temperature and loading speed on interface-dominated strength in fibre/polymer composites: An evaluation for in-situ environment. Mater Des 2015;65:617–26. doi:10.1016/j.matdes.2014.09.053.

[88] Sethi S, Panda PK, Nayak R, Ray BC. Experimental studies on mechanical behavior and microstructural assessment of glass/epoxy composites at low temperatures. J Reinf Plast Compos 2012;31:77–84. doi:10.1177/0731684411431767.

[89] Shukla MJ, Kumar DS, Mahato KK, Rathore DK, Prusty RK, Ray BC. A comparative study of the mechanical performance of glass and glass/carbon hybrid polymer composites at different temperature environments. 4th Natl. Conf. Process. Charact. Mater., 2014. doi:10.1088/1757-899X/75/1/012002.

[90] Surendra Kumar M, Sharma N, Ray BC. Structural integrity of glass/polyester composites at liquid nitrogen temperature. J Reinf Plast Compos 2009;28:1297–304. doi:10.1177/0731684408088889.

[91] Takeda T, Shindo Y, Fukuzaki T, Narita F. Short beam interlaminar shear behavior and electrical resistance-based damage self-sensing of woven carbon/epoxy composite laminates in a cryogenic environment. J Compos Mater 2014;48:119–28. doi:10.1177/0021998312469240.

[92] Miura M, Shindo Y, Takeda T, Narita F. Effect of damage on the interlaminar shear properties of hybrid composite laminates at cryogenic temperatures. Compos Struct 2010;93:124–31. doi:10.1016/j.compstruct.2010.06.008.

[93] Rosenkranz P, Humer K, Weber HW, Pahr DH, Rammerstorfer FG. Static and dynamic scaling experiments on double lap shear specimens at room temperature and at 77 K. Cryogenics 2001;41:21–5. doi:10.1016/S0011-2275(01)00042-X.

[94] Shindo Y, Wang R, Horiguchi K. Analytical and experimental studies of short-beam interlaminar shear strength of G-10CR glass-cloth/epoxy laminates at cryogenic temperatures. J Eng Mater Technol 2002;123:112. doi:10.1115/1.1286235.

[95] Shen XJ, Meng LX, Yan ZY, Sun CJ, Ji YH, Xiao HM, et al. Improved cryogenic interlaminar shear strength of glass fabric/epoxy composites by graphene oxide. Compos Part B Eng 2015;73:126–31. doi:10.1016/j.compositesb.2014.12.023.

[96] Sethi S, Ray BC. An assessment of mechanical behavior and fractography study of glass/epoxy composites at different temperatures and loading speeds. Mater Des 2014;64:160–5. doi:10.1016/j.matdes.2014.07.017.

[97] Delay T, Patterson J, Noorda J. Development of cryogenic composite over-wrapped pressure vessels (COPVS). SAMPE J 2008;3:44–51.

[98] Shindo Y, Miura M, Takeda T, Saito N, Narita F. Cryogenic delamination growth in woven glass/epoxy composite laminates under mixed-mode I/II fatigue loading. Compos Sci Technol 2011;71:647–52. doi:10.1016/j.compscitech.2011.01.006.

[99] Miura M, Shindo Y, Narita F, Watanabe S, Suzuki M. Mode III fatigue delamination growth of glass fiber reinforced polymer woven laminates at cryogenic temperatures. Cryogenics 2009;49:407–12. doi:10.1016/j.cryogenics.2009.05.004.

[100] Takeda T, Miura M, Shindo Y, Narita F. Fatigue delamination growth in woven glass/epoxy composite laminates under mixed-mode II/III loading conditions at cryogenic temperatures. Cryogenics 2013;58:55–61. doi:10.1016/j.cryogenics.2013.10.001.

[101] Soni SM, Gibson RF, Ayorinde EO. The influence of subzero temperatures on fatigue behavior of composite sandwich structures. Compos Sci Technol 2009;69:829–38. doi:10.1016/j.compscitech.2008.02.007.

[102] Shindo Y, Takeda T, Narita F, Saito N, Watanabe S, Sanada K. Delamination growth mechanisms in woven glass fiber reinforced polymer composites under mode II fatigue loading at cryogenic temperatures. Compos Sci Technol 2009;69:1904–11. doi:10.1016/j.compscitech.2009.04.010.

[103] Shindo Y, Takano S, Horiguchi K, Sato T. Cryogenic fatigue behavior of plain weave glass/epoxy composite laminates under tension-tension cycling. Cryogenics 2006;46:794–8. doi:10.1016/j.cryogenics.2006.07.003.

[104] Su X, Abdi F, Kim R. Prediction of micro-crack densities in IM7/977-2 polymer composite laminates under mechanical loading at room and cryogenic temperatures. 46th AIAA/ASME/ASCE/AHS/ASC Struct. Struct. Dyn. Mater. Conf., 2005. doi:10.2514/6.2005-2226.

[105] Donaldson SL, Kim RY. Ply level behavior of carbon/epoxy composites mechanically cycled at cryogenic temperature. 46th AIAA/ASME/ASCE/AHS/ASC Struct. Struct. Dyn. Mater. Conf., 2005. doi:10.2514/6.2005-2159.

[106] Kumagai S, Shindo Y, Inamoto A. Tension-tension fatigue behavior of GFRP woven laminates at low temperatures. Cryogenics 2005;45:123–8.

doi:10.1016/j.cryogenics.2004.06.006.

[107] Donaldson SL, Kim RY. Fatigue of composites at cryogenic temperatures. Int. SAMPE Symp. Exhib., 2002.

[108] Charalambous G, Allegri G, Hallett SR. Temperature effects on mixed mode I/II delamination under quasi-static and fatigue loading of a carbon/epoxy composite. Compos Part A Appl Sci Manuf 2015;77:75–86. doi:10.1016/j.compositesa.2015.05.016.

[109] Shindo Y, Inamoto A, Narita F, Horiguchi K. Mode I fatigue delamination growth in GFRP woven laminates at low temperatures. Eng Fract Mech 2006;73:2080–90. doi:10.1016/j.engfracmech.2006.03.015.

[110] Hartwig G, Hübner R, Knaak S. Fatigue behavior of polymers and composites at cryogenic temperatures. Adv. Cryog. Eng. Mater. Vol. 42A, Springer; 1996. doi:10.1007/978-1-4757-9059-7_21.

[111] Miura M, Shindo Y, Takeda T, Narita F. Mixed-mode I/III fatigue delamination growth in woven glass/epoxy composite laminates at cryogenic temperatures. J Compos Mater 2014;48:1251–9. doi:10.1177/0021998313484951.

[112] Wei Z, Takeda T, Narita F, Shindo Y. Flexural fatigue performance and electrical resistance response of carbon nanotube-based polymer composites at cryogenic temperatures. Cryogenics 2014;59:44–8. doi:10.1016/j.cryogenics.2013.12.004.

[113] Coronado P, Argüelles A, Viña J, Viña I. Influence of low temperatures on the phenomenon of delamination of mode I fracture in carbon-fibre/epoxy composites under fatigue loading. Compos Struct 2014;112:188–93. doi:10.1016/j.compstruct.2014.02.007.

[114] Coronado P, Argüelles A, Viña J, Mollón V, Viña I. Influence of temperature on a carbon-

fibre epoxy composite subjected to static and fatigue loading under mode-I delamination. Int J Solids Struct 2012;49:2934–40. doi:10.1016/j.ijsolstr.2012.05.018.

[115] Shindo Y, Takeda T, Narita F, Yamaki S. Strength characterization of woven glass/epoxy composites under tensile fatigue loading at cryogenic temperatures using open hole specimens. J Compos Mater 2013;47:2885–93. doi:10.1177/0021998312459870.

[116] Shaoquan W, Shangli D, Yu G, Ozbakkaloglu T. Comparison of the mechanical deterioration behavior of C/BMI composite under hygro-thermal or vacuum-thermal cycling. Compos Part A Appl Sci Manuf 2019;119:235–45. doi:10.1016/j.compositesa.2019.02.001.

[117] Park SY, Choi HS, Choi WJ, Kwon H. Effect of vacuum thermal cyclic exposures on unidirectional carbon fiber/epoxy composites for low earth orbit space applications. Compos Part B Eng 2012;43:726–38. doi:10.1016/j.compositesb.2011.03.007.

[118] Gao Y, He S, Yang D, Liu Y, Li Z. Effect of vacuum thermo-cycling on physical properties of unidirectional M40J/AG-80 composites. Compos Part B Eng 2005;36:351–8. doi:10.1016/j.compositesb.2004.10.002.

[119] Yu Q, Chen P, Gao Y, Mu J, Chen Y, Lu C, et al. Effects of vacuum thermal cycling on mechanical and physical properties of high performance carbon/bismaleimide composite. Mater Chem Phys 2011;130:1046–53. doi:10.1016/j.matchemphys.2011.08.033.

[120] Zhang C, Binienda WK, Morscher GN, Martin RE, Kohlman LW. Experimental and FEM study of thermal cycling induced microcracking in carbon/epoxy triaxial braided composites. Compos Part A Appl Sci Manuf 2013;46:34–44. doi:10.1016/j.compositesa.2012.10.006.

[121] Lafarie-Frenot MC, Rouquié S, Ho NQ, Bellenger V. Comparison of damage development in C/epoxy laminates during isothermal ageing or thermal cycling. Compos Part A Appl Sci Manuf 2006;37:662–71. doi:10.1016/j.compositesa.2005.05.002.

[122] Toshiyuki S, Hisaya K, Yasumasa H, Shigeo S, Hiroshi M, Hiroyuki N, et al. Effect of thermal cycling on microcracking and strength degradation of high-temperature polymer composite materials for use in next-generation SST structures. J Compos Mater 2002;36:885–95. doi:10.1106/002199802021469.

[123] Grogan DM, Leen SB, Semprimoschnig COA, Ó Brádaigh CM. Damage characterisation of cryogenically cycled carbon fibre/PEEK laminates. Compos Part A Appl Sci Manuf 2014;66:237–50. doi:10.1016/j.compositesa.2014.08.007.

[124] Flanagan M, Grogan DM, Goggins J, Appel S, Doyle K, Leen SB, et al. Permeability of carbon fibre PEEK composites for cryogenic storage tanks of future space launchers. Compos Part A Appl Sci Manuf 2017;101:173–84. doi:10.1016/j.compositesa.2017.06.013.

[125] Hegde SR, Hojjati M. Effect of core and facesheet thickness on mechanical property of composite sandwich structures subjected to thermal fatigue. Int J Fatigue 2019;127:16–24. doi:10.1016/j.ijfatigue.2019.05.031.

[126] Ju J, Morgan RJ, Creasy TS, Shin EE. Transverse cracking of M40J/PMR-II-50 composites under thermal-mechanical loading: Part II - Experiment and analytical investigation. J Compos Mater 2007;41:1067–86. doi:10.1177/0021998306067260.

[127] Ju J, Morgan RJ, Creasy TS, Shin EE. Transverse cracking of M40J/PMR-II-50 composites under thermal-mechanical loading: Part I - Characterization of main and interaction effects using statistical design of experiments. J Compos Mater 2007;41:1009–31.

doi:10.1177/0021998306067259.

[128] Lundmark P, Varna J. Damage evolution and characterisation of crack types in CF/EP laminates loaded at low temperatures. Eng Fract Mech 2008;75:2631–41. doi:10.1016/j.engfracmech.2007.03.004.

[129] Timmerman JF, Hayes BS, Seferis JC. Cure temperature effects on cryogenic microcracking of polymeric composite materials. Polym Compos 2003;24:132–9. doi:10.1002/pc.10013.

[130] Ju J, Morgan RJ. Characterization of microcrack development in BMI-carbon fiber composite under stress and thermal cycling. J Compos Mater 2004;38:2007–24. doi:10.1177/0021998304044773.

[131] Mizutani Y, Hiratsuka T. Damage analysis of CFRP plates exposed to cryogenic shock by AE monitoring 2005;14:99–111. doi:10.1163/1568551053297094.

[132] Timmerman JF, Tillman MS, Hayes BS, Seferis JC. Matrix and fiber influences on the cryogenic microcracking of carbon fiber/epoxy composites. Compos - Part A Appl Sci Manuf 2002;33:323–9. doi:10.1016/S1359-835X(01)00126-9.

[133] Kobayashi S, Shimpo T, Goto K. Microscopic damage behavior in carbon fiber reinforced plastic laminates for a high accuracy antenna in a satellite under cyclic thermal loading. Adv Compos Mater 2019;28:259–69. doi:10.1080/09243046.2018.1551745.

[134] Timmerman JF, Hayes BS, Seferis JC. Cryogenic microcracking of carbon fiber/epoxy composites: Influences of fiber-matrix adhesion. J Compos Mater 2003;37:1939–50. doi:10.1177/002199803036281.

[135] Jean-St-Laurent M, Dano ML, Potvin MJ. Study of damage induced by extreme thermal cycling in cyanate ester laminates and sandwich panels. J Compos Mater 2017;51:2023–

34. doi:10.1177/0021998316666937.

[136] Yokozeki T, Ishikawa T. Through-thickness connection of matrix cracks in laminate composites for propellant tank. J Spacecr Rockets 2005;42:647–53. doi:10.2514/1.11173.

[137] Bechel VT, Fredin MB, Donaldson SL, Kim RY, Camping JD. Effect of stacking sequence on micro-cracking in a cryogenically cycled carbon/bismaleimide composite. Compos Part A Appl Sci Manuf 2003;34:663–72. doi:10.1016/S1359-835X(03)00054-X.

[138] Kobayashi S, Terada K, Ogihara S, Takeda N. Damage-mechanics analysis of matrix cracking in cross-ply CFRP laminates under thermal fatigue. Compos Sci Technol 2001;61:1735–42. doi:10.1016/S0266-3538(01)00077-X.

[139] Henaff-Gardin C, Lafarie-Frenot MC. Specificity of matrix cracking development in CFRP laminates under mechanical or thermal loadings. Int J Fatigue 2002;24:171–7. doi:10.1016/S0142-1123(01)00070-6.

[140] Mahdavi S, Gupta SK, Hojjati M. Thermal cycling of composite laminates made of out-of-autoclave materials. IEEE J Sel Top Quantum Electron 2018;25:1145–56. doi:10.1515/secm-2017-0132.

[141] Gupta SK, Hojjati M. Thermal cycle effects on laminated composite plates containing voids. J Compos Mater 2019;53:489–501. doi:10.1177/0021998318786785.

[142] Surendra Kumar M, Sharma N, Ray BC. Microstructural and mechanical aspects of carbon/epoxy composites at liquid nitrogen temperature. J Reinf Plast Compos 2009;28:2013–23. doi:10.1177/0731684408090717.

[143] Hui D, Orleans N. Low-temperature and freeze-thaw durability of thick composites. Compos Part B Eng 1996;8368:371–9. doi:10.1016/1359-8368(96)00007-8.

[144] Hegde SR, Hojjati M. Thermally induced microcracks and mechanical property of composite honeycomb sandwich structure: Experiment and finite element analysis. J Sandw Struct Mater 2018. doi:10.1177/1099636218802432.

[145] Lüders C, Sinapius M. Fatigue of fibre-reinforced plastics due to cryogenic thermal cycling. J Compos Mater 2019. doi:10.1177/0021998319826359.

[146] Ajaja J, Barthelat F. Damage accumulation in a carbon fiber fabric reinforced cyanate ester composite subjected to mechanical loading and thermal cycling. Compos Part B Eng 2016;90:523–9. doi:10.1016/j.compositesb.2015.09.054.

[147] He Y, Chen Q, Yang S, Lu C, Feng M, Jiang Y, et al. Micro-crack behavior of carbon fiber reinforced Fe3O4/graphene oxide modified epoxy composites for cryogenic application. Compos Part A Appl Sci Manuf 2018;108:12–22. doi:10.1016/j.compositesa.2018.02.014.

[148] Kim BC, Park SW, Lee DG. Fracture toughness of the nano-particle reinforced epoxy composite. Compos Struct 2008;86:69–77. doi:10.1016/j.compstruct.2008.03.005.

[149] Nishijima S, Honda Y, Okada T. Application of the positron annihilation method for evaluation of organic materials for cryogenic use. Cryogenics 1995;35:779–81. doi:10.1016/0011-2275(95)90913-Z.

[150] Sanada K, Shindo Y. Characterization and modeling of fracture and damage behavior of notched woven fabric GFRP laminates under three-point bending at cryogenic temperatures. J Reinf Plast Compos 2007;26:1429–40. doi:10.1177/0731684407079775.

[151] Sanada K, Shindo Y. Cryogenic damage and fracture behaviors of G-11 woven glass-epoxy laminates. JSME Int J Ser A 2005;48:91–9. doi:10.1299/jsmea.48.91.

[152] Donaldson SL, Kim RY. Compact tension mode I fracture of carbonepoxy and carbon/bismaleimide composites at cryogenic temperatures. 44th AIAA/ASME/ASCE/AHS/ASC Struct. Struct. Dyn. Mater. Conf., 2003. doi:10.2514/6.2003-1431.

[153] Yoshimura A, Takaki T, Noji Y, Yokozeki T, Ogasawara T, Ogihara S. Fracture toughness of CFRP adhesive bonded joints at cryogenic temperature. J Adhes Sci Technol 2012;26:1017–31. doi:10.1163/156856111X593694.

[154] Melcher RJ, Johnson WS. Mode I fracture toughness of an adhesively bonded composite-composite joint in a cryogenic environment. Compos Sci Technol 2007;67:501–6. doi:10.1016/j.compscitech.2006.08.026.

[155] Kim MG, Hong JS, Kang SG, Kim CG. Enhancement of the crack growth resistance of a carbon/epoxy composite by adding multi-walled carbon nanotubes at a cryogenic temperature. Compos Part A Appl Sci Manuf 2008;39:647–54. doi:10.1016/j.compositesa.2007.07.017.

[156] Liu X, Sun T, Wu Z, He H. Mode II interlaminar fracture toughness of unidirectional fiber-reinforced polymer matrix composites with synthetic boehmite nanosheets at room temperature and low temperature. J Compos Mater 2018;52:945–52. doi:10.1177/0021998317716529.

[157] Hojo M, Matsuda S, Fiedler B, Kawada T, Moriya K, Ochiai S, et al. Mode I and II delamination fatigue crack growth behavior of alumina fiber/epoxy laminates in liquid nitrogen. Int J Fatigue 2002;24:109–18. doi:10.1016/S0142-1123(01)00065-2.

[158] Shindo Y, Narita F, Sato T. Analysis of mode II interlaminar fracture and damage behavior in end notched flexure testing of GFRP woven laminates at cryogenic

temperatures. Acta Mech 2006;187:231–40. doi:10.1007/s00707-006-0357-0.

[159] Rizov V, Shindo Y, Horiguchi K, Narita F. Mode III interlaminar fracture behavior of glass fiber reinforced polymer woven laminates at 293 to 4 K. Appl Compos Mater 2006;13:287–304. doi:10.1007/s10443-006-9008-9.

[160] Shindo Y, Takahashi S, Takeda T, Narita F, Watanabe S. Mixed-mode interlaminar fracture and damage characterization in woven fabric-reinforced glass/epoxy composite laminates at cryogenic temperatures using the finite element and improved test methods. Eng Fract Mech 2008;75:5101–12. doi:10.1016/j.engfracmech.2008.07.009.

[161] Miura M, Shindo Y, Takeda T, Narita F. Cryogenic interlaminar fracture properties of woven glass/epoxy composite laminates under mixed-mode I/III loading conditions. Appl Compos Mater 2013;20:587–99. doi:10.1007/s10443-012-9290-7.

[162] Miura M, Shindo Y, Takeda T, Narita F. Interlaminar fracture characterization of woven glass/epoxy composites under mixed-mode II/III loading conditions at cryogenic temperatures. Eng Fract Mech 2012;96:615–25. doi:10.1016/j.engfracmech.2012.09.019.

[163] Shindo Y, Horiguchi K, Wang R, Kudo H. Double cantilever beam measurement and finite element analysis of cryogenic mode I interlaminar fracture toughness of glass-cloth/epoxy laminates. J Eng Mater Technol 2002;123:191. doi:10.1115/1.1345527.

[164] Horiguchi K, Shindo Y, Kudo H, Kumagai S. End-notched flexure testing and analysis of mode II interlaminar fracture behavior of glass-cloth/epoxy laminates at cryogenic temperatures. J Compos Technol Res 2002;24:239–45. doi:10.1520/ctr10930j.

[165] Sumikawa M, Shindo Y, Takeda T, Narita F, Takano S, Sanada K. Analysis of mode I

interlaminar fracture and damage behavior of GFRP woven laminates at cryogenic temperatures. J Compos Mater 2005;39:2053–66. doi:10.1177/0021998305052029.

[166] Shindo Y, Shinohe D, Kumagai S, Horiguchi K. Analysis and testing of mixed-mode interlaminar fracture behavior of glass-cloth⁄epoxy laminates at cryogenic temperatures. J Eng Mater Technol 2005;127:468. doi:10.1115/1.2019944.

[167] Kalarikkal SG, Sankar B V., Ifju PG. Effect of cryogenic temperature on the fracture toughness of graphite/epoxy composites. J Eng Mater Technol 2006;128:151. doi:10.1115/1.2172274.

[168] Aoki T, Ishikawa T, Kumazawa H, Morino Y. Cryogenic mechanical properties of CF/polymer composites for tanks of reusable rockets. Adv Compos Mater 2001;10:349–56. doi:10.1163/156855101753415373.

[169] Choi S, Sankar B V. Fracture toughness of transverse cracks in graphite/epoxy laminates at cryogenic conditions. Compos Part B Eng 2007;38:193–200. doi:10.1016/j.compositesb.2006.06.005.

[170] Oliver MS, Johnson WS. Effect of temperature on mode I interlaminar fracture of IM7/PETI-5 and IM7/977-2 laminates. J Compos Mater 2009;43:1213–9. doi:10.1177/0021998308104147.

[171] López-Puente J, Zaera R, Navarro C. The effect of low temperatures on the intermediate and high velocity impact response of CFRPs. Compos Part B Eng 2002;33:559–66. doi:10.1016/S1359-8368(02)00065-3.

[172] Ohtani K, Numata D, Kikuchi T, Sun M, Takayama K, Togami K. A study of hypervelocity impact on cryogenic materials. Int J Impact Eng 2006;33:555–65. doi:10.1016/j.ijimpeng.2006.09.025.

[173] Shimamoto A, Kubota R, Takayama K. High-velocity impact characteristic of carbon fiber reinforced plastic composite at low temperature. J Strain Anal Eng Des 2012;47:471–9. doi:10.1177/0309324712457125.

[174] Budhoo Y, Delale F, Liaw B. Ballistic impact on woven glass/epoxy composites at high and low temperatures. Proc. 2012 Annu. Conf. Exp. Appl. Mech., 2012. doi:10.1007/978-3-319-62956-8.

[175] Budhoo Y, Delale F, Liaw B. Temperature effect on ballistic impact of woven graphite-epoxy composites. Proc. Soc. Exp. Mech. Ser. 31, 2012. doi:10.1007/978-1-4614-2419-2.

[176] Numata D, Ohtani K, Anyoji M, Takayama K, Togami K, Sun M. HVI tests on CFRP laminates at low temperature. Int J Impact Eng 2008;35:1695–701. doi:10.1016/j.ijimpeng.2008.07.055.

[177] Kim RY, Lee CW, Camping J, Bowman KB. Impact reaction of composites in liquid oxygen. 46th AIAA/ASME/ASCE/AHS/ASC Struct. Struct. Dyn. Mater. Conf., 2005. doi:10.2514/6.2005-2158.

[178] Kim RY, Camping JC, Whitney TJ. Effect of boundary and impact mode on LOX compatibility of graphite composites. 39th Int. SAMPE Tech. Conf., 2007.

[179] Wang G, Li X, Yan R, Xing S. The study on compatibility of polymer matrix resins with liquid oxygen. Mater Sci Eng B Solid-State Mater Adv Technol 2006;132:70–3. doi:10.1016/j.mseb.2006.02.028.

[180] Tudela M, Kim R. Impact damage response of composite materials at LOX/cryogenic temperatures. 46th AIAA/ASME/ASCE/AHS/ASC Struct. Struct. Dyn. Mater. Conf., 2005. doi:10.2514/6.2005-2157.

[181] He YX, Li Q, Kuila T, Kim NH, Jiang T, Lau KT, et al. Micro-crack behavior of carbon fiber reinforced thermoplastic modified epoxy composites for cryogenic applications. Compos Part B Eng 2013;44:533–9. doi:10.1016/j.compositesb.2012.03.014.

[182] Garcia-Gonzalez D, Rodriguez-Millan M, Rusinek A, Arias A. Low temperature effect on impact energy absorption capability of PEEK composites. Compos Struct 2015;134:440–9. doi:10.1016/j.compstruct.2015.08.090.

[183] Khalili SMR, Farsani RE, Soleimani N, Hedayatnasab Z. Charpy impact behavior of clay/basalt fiber-reinforced polypropylene nanocomposites at various temperatures. J Thermoplast Compos Mater 2016;29:1416–28. doi:10.1177/0892705714563561.

[184] Gómez-del Río T, Zaera R, Barbero E, Navarro C. Damage in CFRPs due to low velocity impact at low temperature. Compos Part B Eng 2005;36:41–50. doi:10.1016/j.compositesb.2004.04.003.

[185] Li D sen, Zhao C qi, Jiang N, Jiang L. Experimental study on the charpy impact failure of 3D integrated woven spacer composite at room and liquid nitrogen temperature. Fibers Polym 2015;16:875–82. doi:10.1007/s12221-015-0875-2.

[186] Khan MH, Elamin M, Li B, Tan KT. X-ray micro-computed tomography analysis of impact damage morphology in composite sandwich structures due to cold temperature arctic condition. J Compos Mater 2018;52:3509–22. doi:10.1177/0021998318785671.

[187] Elamin M, Li B, Tan KT. Impact damage of composite sandwich structures in arctic condition. Compos Struct 2018;192:422–33. doi:10.1016/j.compstruct.2018.03.015.

[188] Kara M, Kırıcı M, Tatar AC, Avcı A. Impact behavior of carbon fiber/epoxy composite tubes reinforced with multi-walled carbon nanotubes at cryogenic environment. Compos Part B Eng 2018;145:145–54. doi:10.1016/j.compositesb.2018.03.027.

[189] Li D, Yao Q, Zhao C, Jiang N, Jiang L. Charpy transverse impact failure mechanisms of 3D MWK composites at room and liquid nitrogen temperatures. J Aerosp Eng 2014;28:04014106. doi:10.1061/(asce)as.1943-5525.0000444.

[190] Li D Sen, Jiang N, Zhao CQ, Jiang L, Tan Y. Charpy impact properties and failure mechanism of 3D MWK composites at room and cryogenic temperatures. Cryogenics 2014;62:37–47. doi:10.1016/j.cryogenics.2014.04.007.

[191] Elamin M, Li B, Tan KT. Impact performance of stitched and unstitched composites in extreme low temperature arctic conditions. J Dyn Behav Mater 2018;4:317–27. doi:10.1007/s40870-018-0158-2.

[192] Russo P, Langella A, Papa I, Simeoli G, Lopresto V. Thermoplastic polyurethane/glass fabric composite laminates: Low velocity impact behavior under extreme temperature conditions. Compos Struct 2017;166:146–52. doi:10.1016/j.compstruct.2017.01.054.

[193] Salehi-Khojin A, Bashirzadeh R, Mahinfalah M, Nakhaei-Jazar R. The role of temperature on impact properties of Kevlar/fiberglass composite laminates. Compos Part B Eng 2006;37:593–602. doi:10.1016/j.compositesb.2006.03.009.

[194] Icten BM. Low temperature effect on single and repeated impact behavior of woven glass-epoxy composite plates. J Compos Mater 2015;49:1171–8. doi:10.1177/0021998314531309.

[195] Lopresto V, Papa I, Langella A. Residual strength evaluation after impact tests in extreme temperature conditions. New equipment for CAI tests. Compos Part B Eng 2017;127:44–52. doi:10.1016/j.compositesb.2017.03.013.

[196] Icten BM, Atas C, Aktas M, Karakuzu R. Low temperature effect on impact response of quasi-isotropic glass/epoxy laminated plates. Compos Struct 2009;91:318–23.

doi:10.1016/j.compstruct.2009.05.010.

[197] Ma HL, Jia Z, Lau KT, Leng J, Hui D. Impact properties of glass fiber/epoxy composites at cryogenic environment. Compos Part B Eng 2016;92:210–7. doi:10.1016/j.compositesb.2016.02.013.

[198] Halvorsen A, Salehi-Khojn A, Mahinfalah M, Nakhaei-Jazar R. Temperature effects on the impact behavior of fiberglass and fiberglass/Kevlar sandwich composites. Appl Compos Mater 2006;13:369–83. doi:10.1007/s10443-006-9023-x.

[199] Sánchez-Sáez S, Barbero E, Navarro C. Compressive residual strength at low temperatures of composite laminates subjected to low-velocity impacts. Compos Struct 2008;85:226–32. doi:10.1016/j.compstruct.2007.10.026.

[200] Slifka AJ, Smith DR. Thermal expansion of an E-glass/vinyl ester composite from 4 to 293 K. Int J Thermophys 1997;18:1249–56. doi:10.1007/BF02575259.

[201] Rashkovan IA, Korabel'nikov YG. The effect of fiber surface treatment on its strength and adhesion to the matrix. Compos Sci Technol 1997;57:1017–22. doi:10.1016/S0266-3538(96)00153-4.

[202] Zhang H, Zhang Z, Breidt C. Comparison of short carbon fibre surface treatments on epoxy composites I. Enhancement of the mechanical properties. Compos Sci Technol 2004;64:2021–9. doi:10.1016/j.compscitech.2004.02.009.

[203] Shao Y, Xu F, Liu W, Zhou M, Li W, Hui D, et al. Influence of cryogenic treatment on mechanical and interfacial properties of carbon nanotube fiber/bisphenol-F epoxy composite. Compos Part B Eng 2017;125:195–202. doi:10.1016/j.compositesb.2017.05.077.

[204] Liu W, Gao Y, Liu X, Qiu Y, Xu F. Tensile and interfacial properties of dry-jet wet-spun

and wet-spun polyacrylonitrile-based carbon fibers at cryogenic condition. J Eng Fiber Fabr 2019;14. doi:10.1177/1558925019835164.

[205] Choi S, Sankar B V. Micromechanical analysis of composite laminates at cryogenic temperatures. J Compos Mater 2006;40:1077–91. doi:10.1177/0021998305057365.

[206] Usami S, Ejima H, Suzuki T, Asano K. Cryogenic small-flaw strength and creep deformation of epoxy resins. Cryogenics 1999;39:729–38. doi:10.1016/S0011-2275(99)00084-3.

[207] Kanagaraj S, Pattanayak S. Thermal expansion of glass fabric-epoxy composites at cryogenic temperatures. Int. Cryog. Mater. Conf. 2004, 2004. doi:10.1063/1.1774570.

[208] Su X, Abdi F. Progressive failure analysis of RLV laminates of IM7/PETI-5 - at high, room, and cryogenic temperatures. 44th AIAA/ASME/ASCE/AHS Struct. Struct. Dyn. Mater. Confere, 2003. doi:10.2514/6.2003-1430.

[209] Hartwig G, Hübner R. Thermal and fatigue cycling of fibre composites. Cryogenics 1995;35:727–30. doi:10.1016/0011-2275(95)90900-Z.

[210] Baschek G, Hartwig G. Parameters influencing the thermal expansion of polymers and fibre composites. Cryogenics 1998;38:99–103. doi:10.1016/S0011-2275(97)00117-3.

[211] Wilson PR, Cinar AF, Mostafavi M, Meredith J. Temperature driven failure of carbon epoxy composites – A quantitative full-field study. Compos Sci Technol 2018;155:33–40. doi:10.1016/j.compscitech.2017.11.020.

[212] Lee W, Lee S-B, Yi J-W, Um M-K. Cryogenic thermal expansion properties of carbon fiber reinforced composites. Int. SAMPE Tech. Conf., 2011.

[213] Islam MS, Avila R, Castellanos AG, Prabhakar P. Hybrid textile composites as potential

cryogenic tank materials. 57th AIAA/ASCE/AHS/ASC Struct. Struct. Dyn. Mater. Conf., 2016. doi:10.2514/6.2016-1237.

[214] Praveen RS, Jacob S, Murthy CRL, Balachandran P, Rao YVKS. Hybridization of carbon-glass epoxy composites: An approach to achieve low coefficient of thermal expansion at cryogenic temperatures. Cryogenics 2011;51:95–104. doi:10.1016/j.cryogenics.2010.12.003.

[215] Hartwig G. Extreme properties of fiber composites and their cryogenic applications. Acta Metall Sin 1997;10:283–9.

[216] Gerzeski R. LOX compatible toughened bismaleimide matrix thermally conductive fiber composites Part I: Composite fabrication viability and thermal conductivity measurement. J Test Eval 2008;36:41–54. doi:10.1520/JTE101020.

[217] Ventura G, Martelli V. Very low temperature thermal conductivity of Kevlar 49. Cryogenics 2009;49:376–7. doi:10.1016/j.cryogenics.2009.04.001.

[218] Ventura G, Barucci M, Gottardi E, Peroni I. Low temperature thermal conductivity of Kevlar. Cryogenics 2000;40:489–91. doi:10.1016/S0011-2275(00)00062-X.

[219] Ventura G, Martelli V. Thermal conductivity of Kevlar 49 between 7 and 290 K. Cryogenics 2009;49:735–7. doi:10.1016/j.cryogenics.2009.08.001.

[220] Woodcraft AL, Martelli V, Ventura G. Thermal conductivity of ME771 glass-epoxy laminate from millikelvin temperatures to 4 K. Cryogenics 2010;50:52–4. doi:10.1016/j.cryogenics.2009.10.004.

[221] Wikus P, Figueroa-Feliciano E, Hertel SA, Leman SW, McCarthy KA, Rutherford JM. The thermal conductivity of high modulus Zylon fibers between 400 mK and 4 K. Cryogenics 2008;48:515–7. doi:10.1016/j.cryogenics.2008.07.005.

[222] Martelli V, Ventura G, Micela D. Low temperature thermal conductivity of polymers and composites: Recommended values. 13th Int. Conf. Adv. Technol. Part. Phys., 2012. doi:10.1142/9789814405072_0138.

[223] Runyan MC, Jones WC. Thermal conductivity of thermally-isolating polymeric and composite structural support materials between 0.3 and 4 K. Cryogenics 2008;48:448–54. doi:10.1016/j.cryogenics.2008.06.002.

[224] Kramer E, Kellaris N, Daal M, Sadoulet B, Golwala S, Hollister M. Material selection for cryogenic support structures. J Low Temp Phys 2014;176:1103–8. doi:10.1007/s10909-013-1052-x.

[225] Inoue T, Hayakawa K, Suzuki Y. Thermal conductivity measurement of GFRP at cryogenic temperature. 19th Int. Conf. Compos. Mater., 2013.

[226] Kalaprasad G, Pradeep P, Mathew G, Pavithran C, Thomas S. Thermal conductivity and thermal diffusivity analyses of low-density polyethylene composites reinforced with sisal, glass and intimately mixed sisal/glass fibres. Compos Sci Technol 2000;60:2967–77. doi:10.1016/S0266-3538(00)00162-7.

[227] Evseeva LE, Tanaeva SA. Thermal brhavior of composites containing carbon fibers or nanotubes under cryogenic thermal cycling. Mech Compos Mater 2013;49:155–62. doi:10.1007/s11029-013-9331-9.

[228] Battaglia JL, Saboul M, Pailhes J, Saci A, Kusiak A, Fudym O. Carbon epoxy composites thermal conductivity at 77K and 300K. J Appl Phys 2014;115:1–4. doi:10.1063/1.4882300.

[229] Zhang Z, Klein P, Theiler G, Hübner W. Sliding performance of polymer composites in liquid hydrogen and liquid nitrogen. J Mater Sci 2004;39:2989–95.

doi:10.1023/B:JMSC.0000025824.18291.f0.

[230] Indumathi J, Bijwe J, Ghosh AK, Fahim M, Krishnaraj N. Wear of cryo-treated engineering polymers and composites. Wear 1999;225–229:343–53. doi:10.1016/S0043-1648(99)00063-0.

[231] Hübner W, Gradt T, Schneider T, Börner H. Tribological behaviour of materials at cryogenic temperatures. Wear 1998;216:150–9. doi:10.1016/S0043-1648(97)00187-7.

[232] Wang Q, Zheng F, Wang T. Tribological properties of polymers PI, PTFE and PEEK at cryogenic temperature in vacuum. Cryogenics 2016;75:19–25. doi:10.1016/j.cryogenics.2016.01.001.

[233] Theiler G, Hübner W, Gradt T, Klein P, Friedrich K. Friction and wear of PTFE composites at cryogenic temperatures. Tribol Int 2002;35:449–58. doi:10.1016/S0301-679X(02)00035-X.

[234] Zhang ZZ, Zhang HJ, Guo F, Wang K, Jiang W. Enhanced wear resistance of hybrid PTFE/Kevlar fabric/phenolic composite by cryogenic treatment. J Mater Sci 2009;44:6199–205. doi:10.1007/s10853-009-3862-4.

[235] Theiler G, Gradt T. Friction and wear of polymer materials at cryogenic temperatures. Polym. Cryog. Temp., Springer; 2013, p. 41–59. doi:10.1007/978-3-642-35335-2_3.

[236] Zhang H, Zhang Z. Comparison of short carbon fibre surface treatments on epoxy composites II. Enhancement of the wear resistance. Compos Sci Technol 2004;64:2031–8. doi:10.1016/j.compscitech.2004.02.010.

[237] Rivers HK, Sikora JG, Sankaran SN. Detection of hydrogen leakage in a composite sandwich structure at cryogenic temperature. J Spacecr Rockets 2008;39:452–9. doi:10.2514/2.3829.

[238] Oh BT, Lagoudas DC, Moon S. Mechanical characterization in laminated composite for cryogenic application. Polym Compos 2013;34:607–15. doi:10.1002/pc.22434.

[239] Kumazawa H, Aoki T, Susuki I. Analysis and experiment of gas leakage through composite laminates for propellant tanks. AIAA J 2008;41:2037–44. doi:10.2514/2.1895.

[240] Kumazawa H, Ishikawa T, Suzuki I, Aoki T. Modeling of propellant leakage through matrix cracks in composite laminates. 19th AIAA Appl. Aerodyn. Conf., 2001. doi:10.2514/6.2001-1217.

[241] Peddiraju P, Noh J, Whitcomb J, Lagoudas DC. Prediction of cryogen leak rate through damaged composite laminates. J Compos Mater 2007;41:41–71. doi:10.1177/0021998306063352.

[242] Yokozeki T, Aoki T, Ishikawa T. Experimental cryogenic gas leakage through damaged composite laminates for propellant tank application. J Spacecr Rockets 2005;42:363–6. doi:10.2514/1.13955.

[243] Robinson MJ. Determination of allowable hydrogen permeation rates for launch vehicle propellant tanks. J Spacecr Rockets 2008;45:82–9. doi:10.2514/1.29709.

[244] Grenoble R, Gates T. Hydrogen gas leak rate testing and post-testing assessment of microcrack damaged composite laminates. 47th AIAA/ASME/ASCE/AHS/ASC Struct. Struct. Dyn. Mater. Confere, 2006. doi:10.2514/6.2006-2017.

[245] Grenoble R, Gates T. Hydrogen permeability of polymer matrix composites at cryogenic temperatures. 45th AIAA/ASME/ASCE/AHS/ASC Struct. Struct. Dyn. Mater. Conf., 2005. doi:10.2514/6.2005-2086.

[246] Gates T, Grenoble R, Whitley K. Permeability and life-time durability of polymer matrix

composites for cryogenic fuel tanks. 45th AIAA/ASME/ASCE/AHS/ASC Struct. Struct. Dyn. Mater. Conf., 2004. doi:10.2514/6.2004-1859.

[247] Grogan DM, Leen SB, O. Brádaigh OCM. An XFEM-based methodology for fatigue delamination and permeability of composites. Compos Struct 2014;107:205–18. doi:10.1016/j.compstruct.2013.07.050.

[248] Xu J, Sankar B. Parametric investigation of gas permeability in cross-ply composite laminates using three-dimensional finite elements. 47th AIAA/ASME/ASCE/AHS/ASC Struct. Struct. Dyn. Mater. Confere, 2006. doi:10.2514/6.2006-2093.

[249] Lagoudas D, Peddiraju P, Noh J, Whitcomb J. Numerical modeling of cryogen leakage through composite laminates. 45th AIAA/ASME/ASCE/AHS/ASC Struct. Struct. Dyn. Mater. Conf., 2004. doi:10.2514/6.2004-1862.

[250] Yokozeki T, Ogasawara T, Ishikawa T. Evaluation of gas leakage through composite laminates with multilayer matrix cracks: Cracking angle effects. Compos Sci Technol 2006;66:2815–24. doi:10.1016/j.compscitech.2006.02.024.

[251] Yokozeki T, Ogasawara T, Aoki T, Ishikawa T. Experimental evaluation of gas permeability through damaged composite laminates for cryogenic tank. Compos Sci Technol 2008;69:1334–40. doi:10.1016/j.compscitech.2008.05.019.

[252] Qu X, Venkataraman S, Haftka RT, Johnson TF. Reliability, weight, and cost tradeoffs in the design of composite laminates for cryogenic environments. 42nd AIAA/ASME/ASCE/AHS/ASC Struct. Struct. Dyn. Mater. Conf., 2001. doi:10.2514/6.2001-1327.

[253] Choi S, Sankar B V. Gas permeability of various graphite/epoxy composite laminates for cryogenic storage systems. Compos Part B Eng 2008;39:782–91.

doi:10.1016/j.compositesb.2007.10.010.

[254] Bechel VT, Negilski M, James J. Limiting the permeability of composites for cryogenic applications. Compos Sci Technol 2006;66:2284–95. doi:10.1016/j.compscitech.2005.12.003.

[255] Grogan DM, Ó Brádaigh CM, McGarry JP, Leen SB. Damage and permeability in tape-laid thermoplastic composite cryogenic tanks. Compos Part A Appl Sci Manuf 2015;78:390–402. doi:10.1016/j.compositesa.2015.08.037.

[256] Murray BR, Leen SB, Semprimoschnig COA, Brádaigh CMÓ. Helium permeability of polymer materials as liners for composite overwrapped pressure vessels. J Appl Polym Sci 2016;133:1–10. doi:10.1002/app.43675.

[257] Scatteia L, Lenzi F, Totaro G, Cantoni S, Franceschi M. Composite and nanocomposite materials evaluation and assessment for cryogenic propellant storage. AIAA/CIRA 13th Int. Sp. Planes Hypersonics Syst. Technol., 2015. doi:10.2514/6.2005-3435.

[258] Wei R, Wang X, Chen C, Zhang X, Xu X, Du S. Effect of surface treatment on the interfacial adhesion performance of aluminum foil/CFRP laminates for cryogenic propellant tanks. Mater Des 2017;116:188–98. doi:10.1016/j.matdes.2016.12.011.

[259] Ogasawara T, Arai N, Fukumoto R, Ogawa T, Yokozeki T, Yoshimura A. Titanium alloy foil-inserted carbon fiber/epoxy composites for cryogenic propellant tank application. Adv Compos Mater 2014;23:129–49. doi:10.1080/09243046.2013.844756.

[260] Gates TS, Su X, Abdi F, Odegard GM, Herring HM. Facesheet delamination of composite sandwich materials at cryogenic temperatures. Compos Sci Technol 2006;66:2423–35. doi:10.1016/j.compscitech.2006.01.028.

[261] McVay AC, Johnson WS. Permeability of various hybrid composites subjected to

extreme thermal cycling and low-velocity impacts. J Compos Mater 2010;44:1517–31. doi:10.1177/0021998309353957.

[262] Wilson BA, Technologies WC. Microcracking of carbon fiber composites at cryogenic temperatures. Int. SAMPE Symp. Exhib., 2005.

[263] Choi I, Yu YH, Lee DG. Cryogenic sandwich-type insulation board composed of E-glass/epoxy composite and polymeric foams. Compos Struct 2013;102:61–71. doi:10.1016/j.compstruct.2013.02.017.

[264] Humpenöder J. Gas permeation of fibre reinforced plastics. Cryogenics 1998;38:143–7. doi:10.1016/S0011-2275(97)00125-2.

[265] Sanada K, Sanga H, Shindo Y. Effect of ultrasonication on the cryogenic tensile properties of carbon nanocoil/poly-dicyclopentadiene composites. Compos Part A Appl Sci Manuf 2012;43:1895–900. doi:10.1016/j.compositesa.2012.07.006.

[266] Kim RY, Donaldson SL. Experimental observation of microcracking of composite laminates under cryogenic temperature. AIAA Sp. 2001 Conf. Expo., 2001. doi:10.2514/6.2001-4624.

[267] Lee JK, Song S, Kim B. Functionalized graphene sheets-epoxy based nanocomposite for cryotank composite application. Polym Compos 2012;33:1263–73. doi:10.1002/pc.22251.

[268] Miller S, Meador M. Polymer- layered silicate nanocomposites for cryotank applications. 48th AIAA/ASME/ASCE/AHS/ASC Struct. Struct. Dyn. Mater. Conf., 2007. doi:10.2514/6.2007-2322.

[269] Noorda J, Patterson J, City B, Fronk T, Swenson D. Cryogenic damage tolerance effect on composite materials. Int. SAMPE Symp. Exhib., 2007.

[270] Shindo Y, Takano S, Narita F, Horiguchi K. An experimental - Computational approach to the investigation of tensile properties and damage evolution in woven GFRP laminates at cryogenic temperatures. Mech Adv Mater Struct 2007;14:329–46. doi:10.1080/15376490600910704.

[271] Shindo Y, Fu SY. Testing: Methods for strength characterization of woven fabric composites at cryogenic temperatures. In: Nicolais L, Shindo Y, Fu S-Y, editors. Wiley Encycl. Compos. Second Edi, John Wiley & Sons; 2012, p. 359–67. doi:10.1002/9781118097298.weoc247.

[272] Shindo Y, Watanabe S, Takeda T, Narita F, Matsuda T, Yamaki S. Numerical and experimental evaluation of cryogenic tensile strength of woven fabric-reinforced glass-epoxy composites using open hole specimens. J Mech Mater Struct 2011;6:545–56. doi:10.2140/jomms.2011.6.545.

[273] Pan QY, Fu SY, Zhang YH, Li Y. Measurement of the cryogenic tensile properties of polymer composites. Twent. Int. Cryog. Eng. Conf., 2005.

[274] Rivers HK, Sikora JG, Langley N, Sankaran SN, Rivers HK, Sikora JG, et al. Detection of micro-leaks through complex geometries under mechanical load and at cryogenic temperature. 42nd AIAA/ASME/ASCE/AHS/ASC Struct. Struct. Dyn. Mater. Conf., 2001. doi:10.2514/6.2001-1218.

[275] Yu YH, Nam S, Lee D, Lee DG. Cryogenic impact resistance of chopped fiber reinforced polyurethane foam. Compos Struct 2015;132:12–9. doi:10.1016/j.compstruct.2015.05.021.

[276] Bailey WOS, Bostock TD, Crump DA, Dulieu-barton JM, Robinson AF. Developing a CAI test fixture for consistent testing of composites At teduced temperature. 21st Int. Conf.

Compos. Mater., 2017.

[277] Kim RY, Donaldson SL. Experimental and analytical studies on the damage initiation in composite laminates at cryogenic temperatures. Compos Struct 2006;76:62–6. doi:10.1016/j.compstruct.2006.06.009.

[278] Takeda T, Fan W, Feng QP, Fu SY, Narita F, Shindo Y. Cryogenic mechanical properties of woven glass/epoxy composites modified with multi-walled carbon nanotube and n-butyl glycidyl ether under tensile static and cyclic loadings. Cryogenics 2013;58:33–7. doi:10.1016/j.cryogenics.2013.09.005.